Journal of Medicinal Chemistry

ARTICLE

pubs.acs.org/jmc

N′-(Arylsulfonyl)pyrazoline-1-carboxamidines as Novel, Neutral 5-Hydroxytryptamine 6 Receptor (5-HT$_6$R) Antagonists with Unique Structural Features

Arnold van Loevezijn,* Jennifer Venhorst, Wouter I. Iwema Bakker, Cor G. de Korte, Wouter de Looff, Stefan Verhoog, Jan-Willem van Wees, Martijn van Hoeve,† Rob P. van de Woestijne, Martina A. W. van der Neut, Alice J. M. Borst, Maria J. P. van Dongen, Natasja M. W. J. de Bruin, Hiskias G. Keizer,‡ and Chris G. Kruse

Abbott Healthcare Products B.V. (formerly Solvay Pharmaceuticals B.V.), C. J. van Houtenlaan 36, 1381 CP Weesp, The Netherlands

Supporting Information

ABSTRACT: The 5-HT$_6$ receptor (5-HT$_6$R) has been in the spotlight for several years regarding CNS-related diseases. We set out to discover novel, neutral 5-HT$_6$R antagonists to improve off-target selectivity compared to basic amine-containing scaffolds dominating the field. High-throughput screening identified the *N*′-(sulfonyl)pyrazoline-1-carboxamidine scaffold as a promising neutral core for starting hit-to-lead. Medicinal chemistry, molecular modeling, small molecule NMR and X-ray crystallography were subsequently applied to optimize the leads into antagonists (compounds **1**−**49**) displaying high 5-HT$_6$R affinity with optimal off-target selectivity. Unique structural features include a pseudoaromatic system and an internal hydrogen bond freezing the bioactive conformation. While physicochemical properties and CNS availability were generally favorable, significant efforts had to be made to improve metabolic stability. The optimized structure **42** is an extremely selective, hERG-free, high-affinity 5-HT$_6$R antagonist showing good human in vitro metabolic stability. Rat pharmacokinetic data were sufficiently good to enable further in vivo profiling.

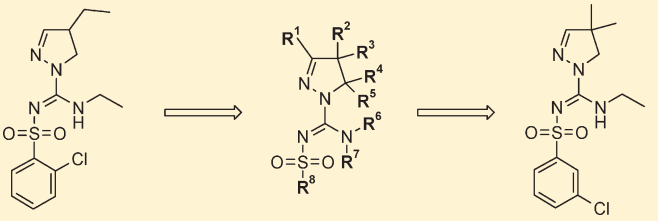

INTRODUCTION

For over a decade, the 5-HT$_6$R has been in the spotlight for central nervous system (CNS) related diseases.[1,2] One apparent reason for this is the observation that the 5-HT$_6$R is mainly (though not exclusively) expressed in the brain.[3,4] Here it indirectly regulates a variety of cholinergic, monoaminergic, and excitatory amino acid neurotransmitters in a brain-region-specific manner.[3,5,6] Although maturing, our understanding of the complex field of 5-HT$_6$R neuropharmacology is neither complete nor fully consistent.[7] With the ambiguous functional role of the 5-HT$_6$R, modulation of this target has been associated with several indications for which unmet medical needs exist.

One of the strongest interests in the 5-HT$_6$R related to CNS disorders today concerns cognitive functions of the brain. In particular, beneficial effects of 5-HT$_6$R antagonism in cognitive impairment (learning and memory deficits) associated with schizophrenia (CIAS) and Alzheimer's disease (AD) are vigorously investigated.[8−17] The downstream signaling pathway(s) and mechanisms involved in cognitive enhancement are yet to be fully elucidated. Acute modulation by the 5-HT$_6$R is believed to occur at least in part through indirect pathways such as disinhibition of GABAergic neurons, leading to brain-region-specific changes in levels of neurotransmitters such as acetylcholine, glutamate, dopamine, and noradrenaline.[3,5,9,15] Additionally, (sub)-chronic treatment with 5-HT$_6$R antagonists has shown effects on synaptic plasticity.[18−20] Such additional effects may make 5-HT$_6$R antagonists a potential procognitive approach that goes beyond a purely symptomatic treatment and may lead to prolonged efficacy in patients.

In clinical studies, 5-HT$_6$R antagonists are evaluated against the currently established treatment of cognitive symptoms in AD, dominated by the acetylcholinesterase inhibitors (AChEIs). The latter compounds are known to lose their efficacy with disease progression, and tolerability is sometimes limited because of cholinergic side effects.[21] The first disclosed results of clinical trials in AD suggest that 5-HT$_6$R antagonist monotherapy in the initial stages of treatment has similar efficacy compared to the AChEI donepezil[22] and seems to be well tolerated. To distinguish 5-HT$_6$R antagonists from established symptomatic AD treatment, it will be interesting to learn whether mechanisms additional to cholinergic modulation will lead to increased or prolonged procognitive efficacy in the various disease stages. Moreover, it remains to be seen whether positive preclinical results in anxiolytic and antidepressive models[23] will translate to additional clinical benefits in these two noncognitive aspects associated with AD. Since the mechanism of action on the cholinergic system is different for 5-HT$_6$R antagonists and AChEIs,

Received: April 18, 2011
Published: August 25, 2011

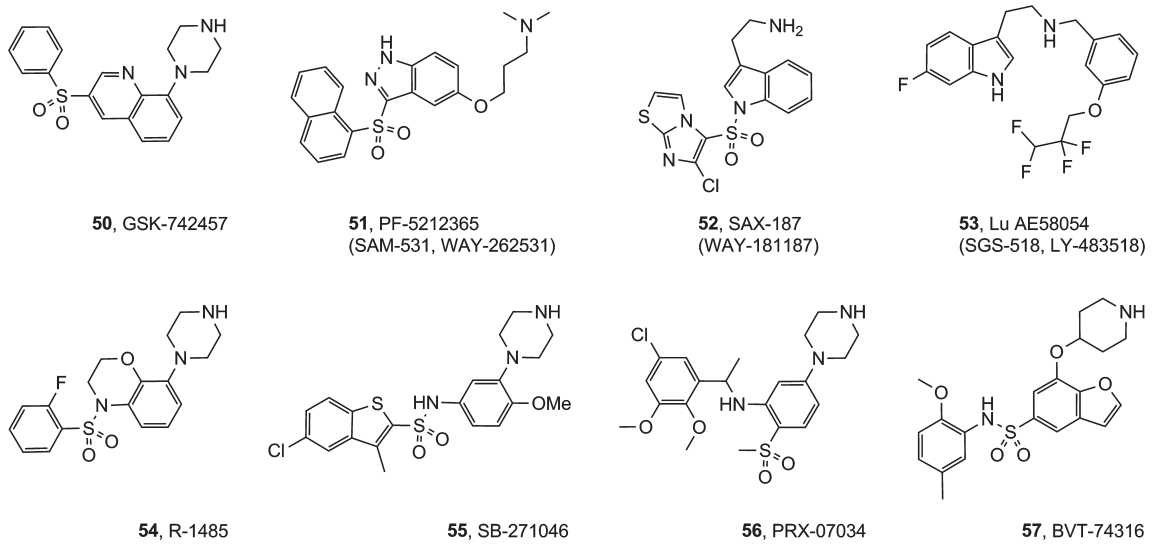

Figure 1. Disclosed structures of 5-HT$_6$R ligands that are or have been under active clinical development (data from Thomson Reuters Integrity).

adjunctive therapy may also be a valuable option. Indeed preclinical data have suggested an additive or synergistic effect,[24−26] and this finding is also receiving clinical follow-up.[27] It may ultimately result in improved efficacy or, in case subefficacious doses of one or both of the individual compounds are used, lead to better tolerability.

In contrast to AD, CIAS is unresponsive to treatment with AChEIs[28] and as such represents a clear unmet medical need.[29] Rather than cholinergic deficits, disturbed dopaminergic and glutamatergic neurotransmission is believed to more strongly underlie CIAS.[30] With the emerging evidence that 5-HT$_6$R antagonism affects multiple neurotransmitters including dopamine and glutamate, this may be a more effective treatment for cognitive symptoms in schizophrenic patients, as also indicated by preliminary clinical studies.[31] However, 5-HT$_6$R antagonists cannot treat the full spectrum of positive and negative symptoms of schizophrenia. Therefore, treatment of CIAS needs to exist as adjunctive therapy with atypical antipsychotics[32] that have a critically balanced target profile. In such a combination treatment, a highly selective 5-HT$_6$R antagonist could be considered preferred. Adjunctive therapy with 5-HT$_6$R antagonists in schizophrenia may have additional benefits beyond cognition. First, schizophrenic patients are known to be more prone to addiction,[33] and 5-HT$_6$R antagonism has been shown to be associated with antiaddictive behavior in several studies.[34−37] Second, atypical antipsychotics are frequently associated with body weight gain,[38] and 5-HT$_6$R modulators have been shown to reduce food intake and body weight in diet-induced obese rodent models, presumably through a centrally mediated effect on satiety.[39,40]

All 14 5-HT receptor family members, except 5-HT$_3$, bear the G-protein-coupled receptor (GPCR) fold with seven characteristic transmembrane helices. The 5-HT$_6$R is further classified as a biogenic amine GPCR because of a conserved aspartic acid in the third transmembrane helix (TM3). In line with the presence of this residue, virtually all 5-HT$_6$R ligands described at the start of our research program contain an interaction counterpart in the form of a basic amine.[41−43] This holds true for all selective 5-HT$_6$R antagonists that are still, or have been, under active clinical development as far as their structures have been disclosed[44] (Figure 1). Few exceptions to this rule hinted at the possibility that neutral compounds may also inhibit this receptor, albeit with apparent lower efficacy.[4] Soon after completion of our 5-HT$_6$R hit finding activities, a higher affinity nonbasic compound was published,[45] but further development of this distinct novel chemotype has not been reported. Only very recently, a few additional publications have appeared that disclose more potent 5-HT$_6$R antagonists lacking a basic amine functionality.[46−50]

Although a protonated amine moiety can demonstrably promote potency of 5-HT$_6$R ligands, its presence may lead to adverse effects in the development stage. Nonselective profiles with respect to both serotonergic subfamily members and other biogenic amine GPCRs are not uncommon.[3] Another liability is the high potential of positively charged ligands for binding to the human ether-a-go-go-related gene (hERG),[51−53] which may translate to QT prolongation and the associated risk of potentially fatal cardiac arrhythmias. This is further heightened by the fact that 5-HT$_6$R ligands generally contain aromatic groups, which represents another pharmacophoric feature of hERG inhibitors. In fact, the 5-HT$_6$R antagonistic framework described in various papers details the presence of two hydrophobic/aromatic groups, linked by a (double) hydrogen bond acceptor moiety and carrying a substituent with a positively ionizable atom.[41,42] Drugs targeting monoaminergic GPCRs in general have an above-average incidence of hERG affinity. For instance, several atypical antipsychotics (targeting a relatively broad spectrum of this class of targets) have been associated with blockade of the hERG channel.[54,55] Combination therapy with 5-HT$_6$R antagonists that would share this liability might increase the incidence of translation to severe cardiac safety risks.

Especially in the light of foreseen adjunctive treatments in CIAS and AD, a high selectivity toward off-targets is of importance to limit disturbance of concurrent therapies and maximize safety. In this study we therefore set out to discover novel, preferably neutral 5-HT$_6$R antagonists to potentially improve off-target selectivity compared to the basic 5-HT$_6$R scaffolds dominating the field. High-throughput screening (HTS) identified the *N*′-(sulfonyl)pyrazoline-1-carboxamidine scaffold as a promising core motif. Here we describe how an integrated approach of medicinal chemistry, molecular modeling, nuclear magnetic resonance (NMR) techniques, and X-ray crystallography

Table 1. In Vitro Pharmacological Results of Hit Compound 1 and Close Analogues

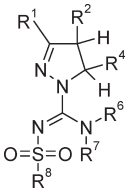

compd	R^1	R^2	R^4	R^6	R^7	R^8	AlogP [a]	K_i (5-HT$_6$), [b] nM	pA_2 (5-HT$_6$) [c]
1	H	C_2H_5	H	C_2H_5	H	2-Cl-phenyl	2.08	27.8 ± 7.7	8.2 ± 0.3
2	H	C_2H_5	H	Bn	H	2-Cl-phenyl	3.32	92.0 ± 22.2	<6.0
3	H	C_2H_5	H	Ph	H	2-Cl-phenyl	3.95	>1000	<6.0
4	H	C_2H_5	H	*i*-C_3H_7	H	2-Cl-phenyl	2.46	>1000	<6.0
5	H	C_2H_5	H	C_2H_5	H	Phenyl	1.42	33.9 ± 8.8	7.8 ± 0.2
6	H	C_2H_5	H	C_2H_5	H	3-Cl-phenyl	2.73	7.9 ± 4.1	8.3 ± 0.1
7	H	C_2H_5	H	C_3H_7	H	3-Cl-phenyl	3.25	14.6 ± 3.5	7.3 ± 0.2
8	H	C_2H_5	H	CH_3	H	3-Cl-phenyl	1.73	17.8 ± 4.0	8.2 ± 0.4
9	H	C_2H_5	H	H	H	3-Cl-phenyl	1.53	24.2 ± 4.6	7.4 ± 0.2
10	H	CH_3	H	C_2H_5	H	3-Cl-phenyl	2.27	8.0 ± 0.1	8.1 ± 1.1
11	H	H	H	C_2H_5	H	3-Cl-phenyl	1.16	33.9 ± 23.0	7.1 ± 0.1
12	CH_3	H	H	C_2H_5	H	3-Cl-phenyl	1.24	231.1 ± 55.9	6.1 ± 0.3
13	H	C_2H_5	H	CH_3	CH_3	3-Cl-phenyl	1.94	>1000	<6.0
14	H	H	Ph	C_2H_5	H	3-Cl-phenyl	3.42	23.9 ± 5.4	7.7 ± 0.1

[a] AlogP was calculated with Pipeline Pilot (Accelrys, Inc.; San Diego, CA, U.S.). [b] Displacement of specific [^{3}H]*N*-methyllysergic acid diethylamide ([^{3}H]LSD) binding in Chinese hamster ovary (CHO) cells stably expressing human 5-HT$_6$ receptor, expressed as K_i ± SEM (nM). [c] Luminescence measurement from a CHO-human-5-HT$_6$-aequorin assay, expressed as pA_2 ± SEM.

was applied to further develop the initial hit structure into a class of high-affinity, CNS druglike 5-HT$_6$R antagonists displaying optimal selectivity toward off-targets.

RESULTS AND DISCUSSION

Hit Identification and Hit-to-Lead Activities. A high-throughput screening campaign was initiated to identify novel antagonists of the 5-HT$_6$R, preferably lacking a basic nitrogen. Screening of a diverse cross-section of our internal compound stock using an in-house 5-HT$_6$R functional assay resulted in a variety of interesting hits belonging to distinct structural classes. Among them, compound **1** sparked immediate interest because of its neutral constituency, leadlike lipophilicity for a CNS drug (AlogP = 2.08) and favorable functional activity, confirmed by a promising result in the receptor binding assay (K_i = 27.8 nM, Table 1) after resynthesis. The identified *N*′-(arylsulfonyl)pyrazoline-1-carboxamidine hit class, sharing its core structure with one of our main classes of CB$_1$ cannabinoid receptor antagonists,[56] provided ample opportunity for structural variation to explore the structure−activity relationships (SARs) (Figure 2).

Initial follow-up on this hit was conducted by exploration of close analogues (Table 1), synthesized according to Scheme 1. Pyrazoline building blocks **60**, with up to one substituent on the C3, C4, and C5 positions, were synthesized from α,β-unsaturated aldehydes or ketones **59** by reaction with hydrazine.[57] Following literature examples[56] these were coupled with *N*-(bismethylsulfanylmethylidene)arylsulfonamides **62**, prepared from their corresponding arylsulfonamides **61**, CS_2, and methyl iodide, to furnish intermediates **63**. Nucleophilic attack of **63** with amines **64** gave target compounds **1**−**14**.

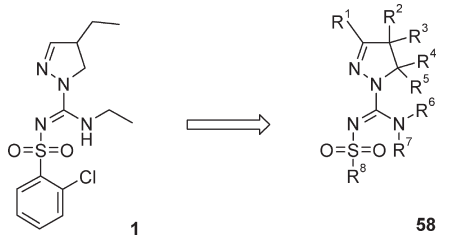

Figure 2. Analogability of identified hit class.

Initial medicinal chemistry efforts focused on varying the R^6 and R^7 N-substituents on the carboxamidine moiety. As evidenced by compounds **2**, **3**, and **4**, substitution of the R^6 ethyl group in **1** by more bulky groups is detrimental for 5-HT$_6$R functional activity. Discrete modifications were subsequently introduced at the R^8 aryl group connected to the sulfonyl moiety. Removal of the 2-chloro atom from the phenyl ring (compound **5**, AlogP reduced to 1.48) only has a marginal effect on the activity and affinity compared to **1**. In contrast, the 3-chlorophenyl substitution in compound **6** (AlogP = 2.73) showed a more than 3-fold increase in affinity. In combination with this R^8 substituent, additional R^6 variations with both elongation (**7**) and shortening (**8** and **9**) of the *N*-ethyl group were investigated. Neither strategy resulted in improved 5-HT$_6$R antagonism. Subsequently, the effects of differential substitution of the pyrazoline ring were studied. In the obtained racemic mixtures, reducing the ethyl R^2 substituent of **6** to a methyl in **10** only had a marginal effect. However, complete eradication of this group (**11**) resulted in a sharp drop in both receptor binding and functional activity. Introduction of even a small methyl R^1

dx.doi.org/10.1021/jm200466r |*J. Med. Chem.* 2011, 54, 7030–7054

Scheme 1. Synthesis of Initial Hit Exploration Compounds[a]

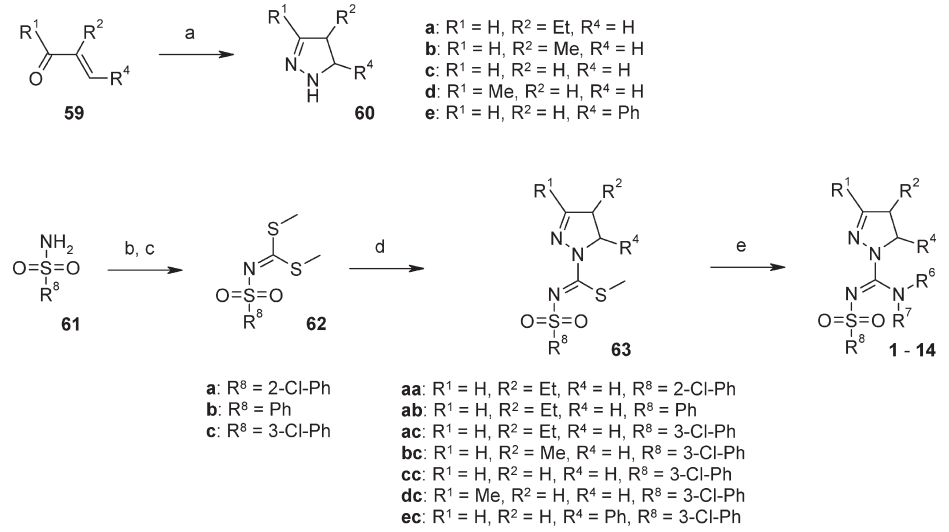

[a] Reagents and conditions: (a) $H_2NNH_2 \cdot H_2O$, MeOH or CH_3CN, 0 °C to room temp [R^4 = H] or $H_2NNH_2 \cdot H_2O$, *t*-BuOH, reflux [R^4 = Ph]; (b) CS_2, KOH, DMF/H_2O, 10 °C; (c) MeI, 10 °C to room temp; (d) **60**, pyridine, reflux; (e) R^6R^7NH [**64**, R^6,$R^7 \neq$ Ar], MeOH, room temp or R^6R^7NH [**64**, R^6 = Ph, R^7 = H], NaHMDS, THF, 0 °C to room temp.

Scheme 2. Alternative Route Used for Synthesis of *N*′-(Acyl)pyrazoline-1-carboxamidine Analogue 15[a]

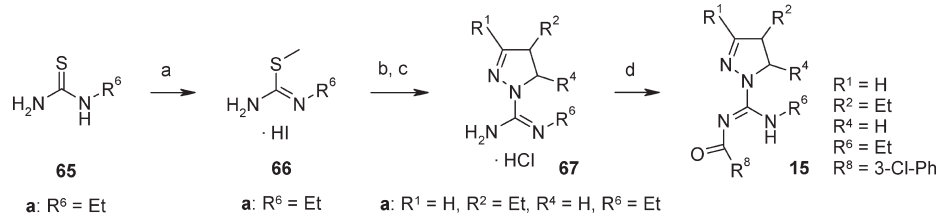

[a] Reagents and conditions: (a) MeI, EtOH, 0 °C to room temp; (b) **60**, DiPEA, toluene, reflux; (c) HCl, EtOH, room temp; (d) R^8COCl, DiPEA, CH_2Cl_2, room temp.

substituent, evidenced by compound **12**, resulted in a marked loss of activity. Compared to **8**, replacement of the R^7 hydrogen by a methyl substituent (**13**) led to a dramatic decrease in activity. Finally, the so far untouched C5-position of the pyrazoline ring was probed by introduction of an aryl functionality (R^4 = Ph). For the racemic mixture (**14**) this resulted in interesting pharmacodynamic properties and as such identification of another subseries with potential for further lead optimization, albeit with a rather high AlogP (3.42).

To conclude the initial SAR studies, a single attempt was made to replace the sulfonyl moiety in lead optimization candidate **6** by a carbonyl group. Synthesis was achieved via an alternative route, based on literature precedent[56] with slight modifications, as depicted in Scheme 2. Thiourea **65a** was methylated to furnish a suitable leaving group in *S*-methylisothiourea **66a**, which could be substituted with pyrazoline building block **60a** to give the pyrazoline-1-carboxamidine core **67a**. Regioselective acylation of the **67a** with 3-chlorobenzoyl chloride gave target compound **15**. Its lack of 5-HT_6R affinity (K_i > 1000 nM) and functional activity (pA_2 < 6) demonstrated the importance of the sulfonyl linker, as seen in numerous 5-HT_6R ligands.

As compounds **6** (pyrazoline 4-alkyl subseries) and **14** (pyrazoline 5-aryl subseries) elicited the most favorable profiles in terms of 5-HT_6R affinity and antagonistic potency in the hit exploration study, some additional profiling of these compounds was performed. As anticipated because of the absence of a basic nitrogen,[58] both are devoid of hERG affinity with pIC_{50} < 5 measured at Zenas.[59] Screening against a panel of 40 targets at Cerep,[60] dominated by monoaminergic GPCRs including homologous human 5-HT receptor subtypes 1A, 1D, 2A, 2C, and 7, and the human D_2 receptor, additionally showed that these lead compounds are highly specific for the 5-HT_6R with all measured off-target K_i > 1000 nM (see Supporting Information for full data). Notably, despite an identical core structure and substitution on the arylsulfonyl and guanidine N highly similar to our previously disclosed CB_1 antagonists,[56] high selectivity against the CB_1 receptor was also observed. This is due to the fact that for CB_1 affinity aryl substituents on both the pyrazoline C3 (R^1) and C4 (R^2) positions are a prerequisite. The high membrane passage of **6** and **14** (39.8 and 38.5%, respectively, likely aided by their nonionizable character) and their low P-glycoprotein mediated efflux (P-gp factor 1.0 and 1.4, respectively) were also favorable. However, both compounds were found to have quite low metabolic stability in both human (Cl_{int} of 53 and 73 (μL/min)/10^6 cells, respectively) and rat (Cl_{int} of 92 and 116 (μL/min)/10^6 cells, respectively) hepatocytes. As such, improving this was an issue requiring rigorous investigation in follow-on lead optimization.

dx.doi.org/10.1021/jm200466r |*J. Med. Chem.* 2011, 54, 7030–7054

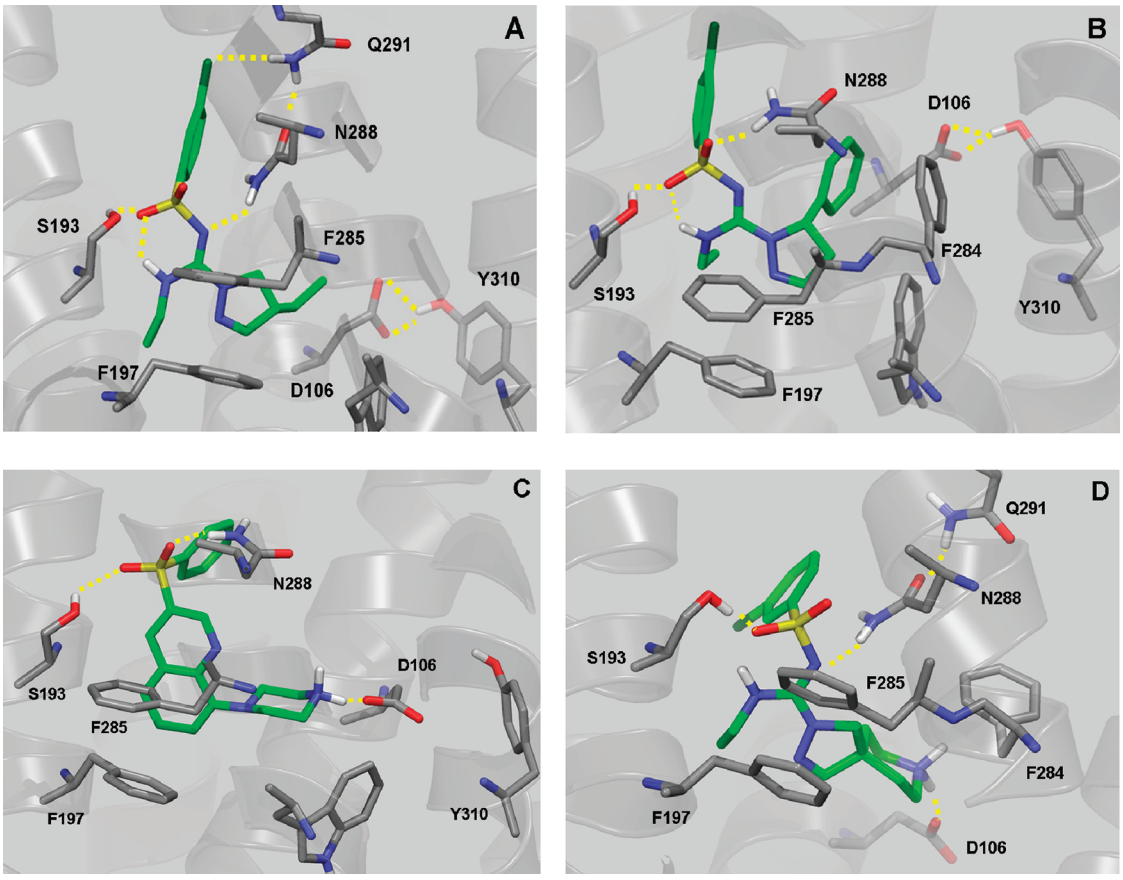

Figure 3. Docking poses of 5-HT$_6$R antagonists: (A) compound **6**; (B) (*S*)-isomer of compound **14**; (C) compound **50** (GSK-742457); (D) compound **47**. Conserved interactions featured by all ligands involve hydrogen bonds (shown in yellow dotted lines) with S193 and N288. The basic antagonists **50** and **47** furthermore engage in a salt bridge with D106, which is conserved in biogenic GPCRs. The neutral ligands in contrast display π-stacking and/or hydrophobic interactions with residues in the hydrophobic pocket, which is formed when D106 adopts the gauche$^+$ conformation. In this conformation D106 is "neutralized" by Y310. Notably, the latter interaction (including a ligand salt bridge with the conserved aspartate) has also been observed for corresponding residues in crystallized GPCR complexes with basic compounds, e.g., carazolol and timolol bound to the β_2-adrenergic receptor (PDB codes 2RH1 and 3D4S).[61] Ballesteros numbering of the featured residues is the following: D106/D3.32; S193/S5.43; F197/F5.46; F284/F6.51; F285/F6.52; N288/N6.55; Q291/Q6.58; Y310/Y7.43.

Design. In the next step we strived to better understand the limited SAR around the *N*′-(sulfonyl)pyrazoline-1-carboxamidine core obtained thus far. To take optimal advantage of unexplored optimization opportunities, we engaged in docking studies using a 5-HT$_6$R homology model (see Experimental Section for details). Particular points of interest to address included the site and mode of binding compared to ionizable reference structures and the nature of the interactions resulting in the somewhat unexpected high binding affinity observed for this neutral class.

Docking studies of representatives from the series showed striking features, illustrated by compounds **6** and **14** in Figure 3A and Figure 3B. The binding site of the *N*′-(arylsulfonyl)pyrazoline-1-carboxamidines almost entirely overlaps with that of ionizable 5-HT$_6$R antagonists such as 3-benzenesulfonyl-8-piperazin-1-yl-quinoline (GSK-742457, **50**) currently in clinical phase II (Figure 3C). Common interaction residues include serine-193 (S193) and asparagine-288 (N288). Both residues hydrogen-bond to the sulfonyl moiety of **50**. In the case of **6** and **14**, S193 similarly hydrogen-bonds to the sulfonyl group. Residue N288, however, is able to interact with both the sulfonyl oxygen and amide lone pair of the compounds. Interestingly, the 3-chloro substituent in **6** is able to engage in polar interaction with glutamine-291 (Q291), which in turn stabilizes N288. This is nicely in line with the observed decrease in K_i of **6** compared to the unsubstituted and 2-chloro substituted phenyl analogues **5** and **1**. This polar interaction is not present in the 5-aryl substituted pyrazoline, compound **14**. The introduction of the bulky R^4 group requires small reorientations of the structure in the binding pocket compared to **6**, thus moving the 3-chloro substituent on the R^8 phenyl ring further away from Q291. The absence of this polar interaction is however compensated by π-stacking interactions of the R^4-aryl group with phenylalanine-284 (F284). This was only observed for the (*S*)-isomer; the (*R*)-isomer could not be docked because of steric restrictions. In contrast, compound **6** with its R^2 ethyl substituent on the pyrazoline 4-position could be docked in both configurations without preference.

A notably conserved interaction is the π-stacking interaction with phenylalanine-285 (F285), held in place by phenylalanine-197 (F197). Where **50** optimally positions its quinoline moiety for stacking interactions, a pseudoaromatic system is formed by the conjugated pyrazoline-1-carboxamidine moiety of **6** and **14**, satisfying the same molecular interactions. Another prominent feature of active members from the *N*′-(arylsulfonyl)pyrazoline-1-carboxamidine structural class, deduced from docking studies,

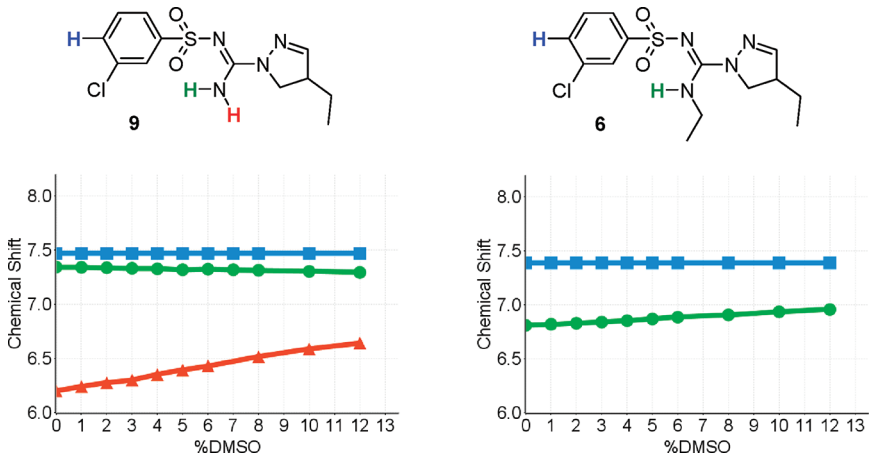

Figure 4. Change in chemical shift of the carboxamidine NH protons, and a reference proton, as a result of titration with DMSO. Illustrated are the $\Delta\delta$ values observed for **9** and **6** of the para proton of the phenylsulfonyl group (blue), the carboxamidine NH hydrogen (R^7) bonded to the sulfonyl group (green), and a free carboxamidine NH (R^6) in **9** (red).

is the presence of an internal hydrogen bond in a six-membered ring topology[62] between the R^7 hydrogen substituent and one of the sulfonyl oxygens. This intramolecular interaction stabilizes the bioactive conformation, and the resulting favorable entropy contribution adds to the high affinity of this structural class despite the absence of a basic nitrogen. The latter, when present, interacts with aspartate-106 (D106) through a salt bridge as illustrated in Figure 3C for **50**. In the case of the neutral *N*′-(arylsulfonyl)pyrazoline-1-carboxamidines, D106 has changed rotamers from the trans to the gauche$^+$ conformation. In this conformation the negative charge is facing away from the antagonist and toward tyrosine-310 (Y310), with which it forms an alternative hydrogen bond. A hydrophobic pocket is thus shaped to accommodate apolar groups from the ligands. As illustrated by **11**, **10**, and **6**, increasing the size of the aliphatic R^2 substituent indeed provides an opportunity to increase ligand affinity via additional hydrophobic interactions. The low affinity of compound **13** is also in line with modeling efforts, as the presence of both an R^6 and an R^7 alkyl substituent precludes intramolecular hydrogen bond formation with the sulfonyl group that stabilizes the bioactive conformation.

Validation of the Binding Mode Hypothesis by Ligand-Based NMR and X-ray Diffraction. The characteristic intramolecular hydrogen bond featured in the binding poses of the *N*′-(arylsulfonyl)pyrazoline-1-carboxamidines prompted us to investigate whether this interaction can be measured in solution by NMR. If detectable, it would indicate this internal interaction to be highly favorable and to result in a low energy conformation.

Several representative compounds were used to study the change in shift ($\Delta\delta$) of an NH peak upon addition of dimethylsulfoxide (DMSO).[63] Any type of hydrogen bonding of the studied compound with DMSO will result in deshielding of the bonded proton. Therefore, a downfield shifted proton resonance upon titration with DMSO indicates increased hydrogen bonding character of the compound NH with DMSO. A strongly hydrogen-bonded NH, such as in the hypothesized internal hydrogen bond, will already show the upfield shift and will resist solvation by DMSO. An observed small $\Delta\delta$ for the compound's NH thus confirms the existence of an internal hydrogen bond. As shown in Figure 4, compound **9** contains two NH peaks. One is solvatable, showing a large downfield shift upon DMSO titration, while the other is clearly bound. For comparison, the shift of the para-phenyl proton is shown as well. Compound **6** also displays little solvation, indicating its NH to be already engaged in quite a strong hydrogen bonding interaction. Additionally studied analogues with a single carboxamidine NH proton displayed the same pattern (data not shown). One may argue that the internal hydrogen bond can alternatively involve the N atom at position 2 in the pyrazoline ring instead of the sulfonyl oxygen. To exclude this possibility, an analogue lacking this possible interaction was also studied (pyrazoline replaced by 2-aza-bicyclo[2.2.2]octane). This again resulted in a similar pattern (data not shown), confirming that the hydrogen bond interaction occurs between the sulfonyl oxygen and carboxamidine NH.

The homology model predicted only the (*S*)-enantiomer of **14** to be active. As an additional check for the binding mode hypothesis, racemic **14** was separated by chiral preparative high performance liquid chromatography (HPLC) into its two enantiomers **16** and **17** and tested in the 5-HT_6 receptor binding and functional assays (Table 2). The (−)-isomer **16** was shown to be active, whereas the (+)-isomer **17** was inactive. Crystallization attempts were carried out for both enantiomers, and the crystals of the inactive (+)-enantiomer **17** were of suitable quality for X-ray diffraction. Both the Flack *x* parameter[64] value (−0.02 ± 0.004) and the independent analysis of the data in terms of the Hooft parameter[65] (−0.002 ± 0.012) indicated an enantiomerically pure structure of **17** with a high level of confidence. As depicted in Figure 5, the chiral carbon in **17** proved to have the (*R*)-configuration. This means that, in line with the predictions from the protein model, the active (−)-enantiomer **16** has the (*S*) absolute stereochemistry. Interestingly, the crystal structure of **17** features the same internal hydrogen bond found by NMR and docking studies, again indicating this to be an abundantly populated conformation for this structural class.

Weak Spot Analysis. Metabolic stability was identified as an issue for further optimization, based on the early ADME (absorption, distribution, metabolism, and excretion) properties of leads **6** and **14**. Therefore, weak spot predictions were used to steer compound optimization using the application MetaSite.[66] First, both compounds were profiled in a cytochrome P450 (CYP) reaction phenotyping assay at Cyprotex[67] to identify which of the main CYP isoforms were major metabolizers.

Table 2. In Vitro Pharmacological Results of the 5-Aryl Substituted Pyrazolines

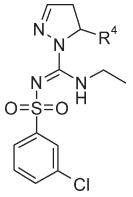

compd	R^4	AlogP [a]	K_i (5-HT$_6$),[b] nM	pA_2 (5-HT$_6$),[c]	Cl$_{int}$, human,[d]	Cl$_{int}$, rat,[d]
14 racemate	phenyl	3.42	23.9 ± 5.4	7.7 ± 0.1	73	116
16 (*S*)-(−)-enantiomer	phenyl	3.42	9.3 ± 3.5	8.0 ± 0.2	107	116
17 (*R*)-(+)-enantiomer	phenyl	3.42	>1000	<6.0	ND	107
18 racemate	pyridin-4-yl	2.27	321.8 ± 42.5	6.9 ± 0.4	50	87
19 racemate	furan-2-yl	2.06	8.2 ± 2.5	8.1 ± 0.1	92	198
20 racemate	4-F-phenyl	2.98	138.1 ± 43.1	6.4 ± 0.1	107	126

[a] AlogP was calculated with Pipeline Pilot (Accelrys, Inc.; San Diego, CA, U.S.). [b] Displacement of specific [^{3}H]*N*-methyllysergic acid diethylamide ([^{3}H]-LSD) binding in CHO cells stably expressing human 5-HT$_6$ receptor, expressed as K_i ± SEM (nM). [c] Luminescence measurement from a CHO-human-5-HT$_6$-aequorin assay, expressed as pA_2 ± SEM. [d] In vitro intrinsic clearance from hepatocyte assay [(μL/min)/10^6 cells].

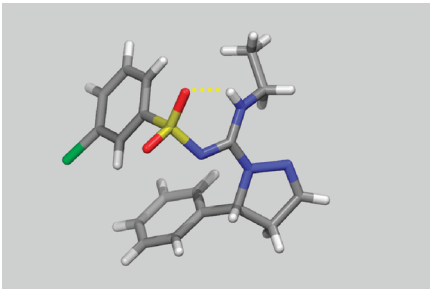

Figure 5. X-ray structure of **17**, the (*R*)-isomer of racemic **14**, featuring the internal hydrogen bond indicated by docking to be present in the bioactive conformation of this compound.

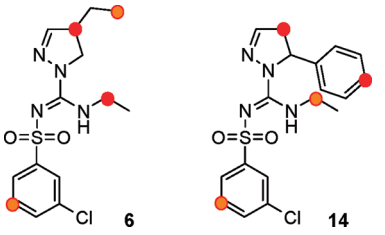

Figure 6. Prominent metabolic weak spots of **6** and **14** predicted by MetaSite's 2C19 and 3A4 models.

In either case, this proved to be CYP 2C19 and CYP 3A4. We thus focused on MetaSite's rankings for these specific isoforms. The most highly ranked weak spots from the MetaSite prediction are depicted in Figure 6.

For **6** the weak spots amenable for further optimization included the R^8 aryl substituent on the sulfonyl moiety, the R^6 carboxamidine *N*-ethyl group, the C4-position of the pyrazoline ring, and the R^2 alkyl substituent attached to this position. According to the docking studies, ample room for additional substitution is available at the R^8 and R^2 positions. These positions thus warranted extensive further exploration while trying to avoid rigorous rises in lipophilicity (**6**, AlogP = 2.73) and polar surface area (**6**, PSA = 82 Å^2) that would endanger CNS availability. Given that both initial SAR and docking studies indicated limited substitution possibilities in groups at the R^6 position, only discrete variations were considered here. But first, the 5-aryl substituted analogue **14** (AlogP = 3.42, PSA = 82 Å^2), with its bulkier R^4 substitution at the pyrazoline C5 position, was further explored.

Lead Optimization: Pyrazoline 5-Aryl Substitution. Chiral separation of **14** showed that the active (*S*)-(−)-enantiomer **16** displayed good activity toward the 5-HT$_6$R with a K_i of 9.3 nM and a pA_2 of 8.0, whereas the (*R*)-(+)-enantiomer **17** was inactive (Table 2). Moreover, no significant difference in metabolic stability between the racemate and its two pure enantiomers was observed. Therefore, to evaluate the R^4 modifications, it was felt that screening of racemic mixtures would suffice. In order to investigate whether modifications in the pyrazoline C5-position would produce more stable and/or more active compounds, several analogues with the R^4 phenyl substituent replaced by a five- or six-membered heteroaryl group were prepared. The latter analogues are represented in Table 2 by compounds **18** (AlogP = 2.27) and **19** (AlogP = 2.06), which have reduced lipophilicity compared to **14** (AlogP = 3.42). In **18**, one of the highly ranked weak spots by MetaSite (the para position of the phenyl ring) is directly modified by replacing the CH for an N. In addition, we tried to block this predicted weak spot by introducing a fluoro substituent on the ring (compound **20**, AlogP = 2.98). These test compounds were synthesized through the intermediates depicted in Scheme 3. The followed route is analogous to the general one depicted in Scheme 1. If the required α,β-unsaturated aldehyde substrate **59** (R^1 = R^2 = H) was not commercially available, it was synthesized from the R^4-aldehyde **68** via a Wittig-type reaction.[68]

Both replacement of the phenyl by a 4-pyridyl or a 4-fluorophenyl ring had a strong detrimental impact on 5-HT$_6$R affinity and activity, whereas metabolic stability did not improve significantly. The phenyl to 2-furyl replacement in compound **19** resulted in retained 5-HT$_6$R activity, although without any sign of improved resistance despite a marked reduction in lipophilicity. This series was therefore abandoned, and attention was refocused on modifications in the guanidine *N*-alkyl, arylsulfonyl, and pyrazoline C4 substituents.

Lead Optimization: *N*-Alkyl Substitutions. Early SAR studies involving R^6 demonstrated that the carboxamidine *N*-ethyl

Scheme 3. Synthesis of Pyrazoline C5 (Hetero)aryl Analogues[a]

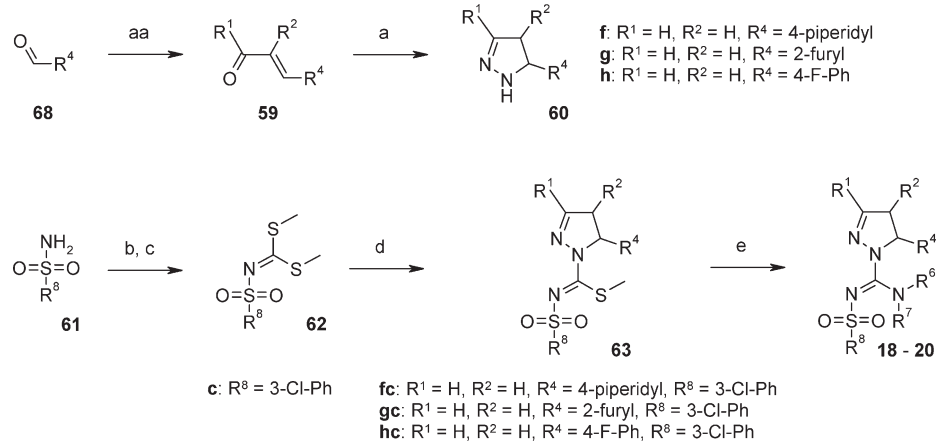

[a] Reagents and conditions: (aa) $Ph_3P{=}CH{-}CHO$, DMF, room temp; (a) $H_2NNH_2 \cdot H_2O$, *t*-BuOH, reflux [R^4 = 2-furyl] or $H_2NNH_2 \cdot H_2O$, Et_2O or THF, −10 °C to room temp [R^4 = 4-piperidyl or 4-F-Ph]; (b) CS_2, KOH, DMF/H_2O, 10 °C; (c) MeI, 10 °C to room temp; (d) **60**, pyridine, 60 °C or reflux; (e) $EtNH_2$ [**64**, R^6 = Et, R^7 = H], MeOH, room temp.

Scheme 4. Synthesis of Carboxamidine NH-R^6 Analogues[a]

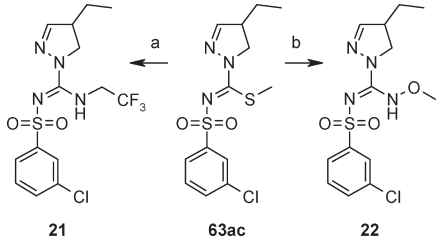

[a] Reagents and conditions: (a) $CF_3CH_2NH_2$, MeOH, 60 °C (sealed tube); (b) $CH_3ONH_2 \cdot HCl$, Et_3N, MeOH, 50 °C.

substituent was most favorable for 5-HT_6R affinity and potency (Table 1). At the same time, however, this group constitutes a weak spot. Hydroxylation at the α-position as predicted by MetaSite (Figure 6) would lead to N-dealkylation. Indeed incubation of **6** with human hepatocytes led to clearly detectable levels of the *N*-desethyl analogue **9** (data not shown). Although this metabolite is active, it is less potent than the parent compound. We therefore attempted some final modifications of the α- and β-positions of the *N*-ethyl substituent to modulate the rate of metabolism (Scheme 4).

Substitution of the terminal carbon atom with three fluorines (**21**, AlogP = 2.74) resulted in a marked reduction in receptor binding and functional activity (K_i = 189.4 ± 30.9 nM; pA_2 = 7.0 ± 0.1), whereas compared to **6**, no improvement in metabolic stability was observed (Cl_{int} of 43 and 99 (μL/min)/10^6 cells in human and rat hepatocytes, respectively). Modification of the α-position by going to the *N*-methoxy derivative **22** (AlogP = 2.22) was found to be detrimental for 5-HT_6R activity (K_i = 297.5 ± 137.7 nM; pA_2 < 6). With our attempts being unsuccessful and further options being limited because of steric restraints, this line of SAR exploration was terminated.

Lead Optimization: Arylsulfonyl Substitutions. As compound **6** still proved to be the best lead so far, this structure was used as the basis for further optimization focused on the arylsulfonyl moiety. Several analogues were specifically synthesized to address weak spots on the R^8 phenyl ring, whereas others were part of a broader SAR exploration also covering heteroaromatic moieties. A wide range of variations was introduced with a representative selection listed in Table 3. These include several bicyclic (hetero)aromatic ring systems that could be accommodated by our 5-HT_6R homology model. As set out in Scheme 5, these compounds are accessible via two distinct routes. The first option is essentially the strategy as followed in Scheme 1, in which the R^8 arylsulfonyl substituent is introduced early in the route. Options are left for diversification with different pyrazoline and amine building blocks in a later stage. This strategy was for example chosen to evaluate arylsulfonyl substituents present in basic competitor 5-HT_6R modulators, such as SB-271046 (**55**) and WAY-181187 (**52**) leading to analogues **35** and **36**, respectively. However, in this case a more prominent need to introduce diversity in the R^8 substituent as late as possible in the route existed. We therefore also developed a suitable parallel synthesis approach complying with these criteria. Analogous to the acylation reaction set out in Scheme 2, it was found that reaction of **67a** with arylsulfonyl chlorides under mild conditions led to formation of the target compounds in a highly regiospecific manner. The neutral character of the products allowed a suitable parallel workup procedure. Extraction of the reaction mixture with 2 N aqueous NaOH quenched any remaining sulfonyl chloride, removing the sulfonic acids into the aqueous layer. Subsequent SPE purification of the organic phase over strong cation exchange (SCX) columns caught any remaining basic core **67a** while eluting the neutral products. With a few exceptions, the target compounds were directly obtained from evaporation without the need for further purification.

Overall it can be concluded that quite substantial variations in R^8 are tolerated, without dramatic loss or gain of 5-HT_6R activity. This concurs with docking studies, as does the observation that the 3-chloro atom of **6** fulfills a particular role in 5-HT_6R binding (Figure 3A). All other monosubstitutions introduced at the phenylsulfonyl 3-position (**24**−**27**) exhibited lower activity toward the 5-HT_6R and at best slightly improved human but similar rat metabolic stability. Moving the chloro substituent from the 3- to the 4-position (**23**) was allowed but without obvious benefit. Introduction of an additional chloro substituent onto **6** only had a positive effect on 5-HT_6R activity when placed at the 4-position (**28**, rise of AlogP to 3.39) but rendered the

dx.doi.org/10.1021/jm200466r |*J. Med. Chem.* 2011, 54, 7030–7054

Table 3. In vitro Pharmacological Results of the Arylsulfonyl SAR and Metabolic Stability studies

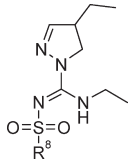

compd	R^8	AlogP [a]	K_i (5-HT_6), [b] nM	pA_2 (5-HT_6), [c]	Cl_{int}, human, [d]	Cl_{int}, rat, [d]
1	2-Cl-phenyl	2.08	27.8 ± 7.7	8.2 ± 0.3	39	99
6	3-Cl-phenyl	2.73	7.9 ± 4.1	8.3 ± 0.1	53	92
23	4-Cl-phenyl	2.73	18.5 ± 7.0	8.2 ± 0.3	40	99
24	3-F-phenyl	1.62	17.0 ± 4.4	7.9 ± 0.1	33	116
25	3-CF_3-phenyl	2.36	17.9 ± 7.4	7.5 ± 0.3	27	116
26	3-Me-phenyl	1.90	27.4 ± 7.5	7.1 ± 0.2	51	116
27	3-MeO-phenyl	1.40	26.6 ± 6.6	7.0 ± 0.3	46	92
28	3,4-di-Cl-phenyl	3.39	7.9 ± 0.0	8.9 ± 0.1	92	198
29	3,5-di-Cl-phenyl	2.75	21.9 ± 9.1	7.6 ± 0.2	139	126
30	2,5-di-Cl-phenyl	2.75	119.4 ± 6.5	7.0 ± 0.0	ND	116
31	2,6-di-Cl-phenyl	2.75	196.7 ± 32.2	6.8 ± 0.1	ND	126
32	2-F-3-Cl-phenyl	2.29	2.7 ± 0.2	8.1 ± 0.2	36	116
33	1-naphthyl	2.97	5.6 ± 1.5	8.6 ± 0.3	77	154
34	2-naphthyl	2.32	17.2 ± 7.2	8.1 ± 0.1	41	139
35	5-chloro-3-methylbenzo[*b*]thiophen-2-yl	4.20	8.5 ± 2.2	8.1 ± 0.1	82	154
36	6-chloroimidazo[2,1-*b*]thiazol-5-yl	1.95	7.9 ± 4.2	8.0 ± 0.2	20	116
37	5-chlorothiophen-2-yl	1.66	4.1 ± 2.0	8.5 ± 0.2	39	126
38	5-chloro-1,3-dimethyl-1*H*-pyrazol-4-yl	0.81	510.1 ± 67.4	6.9 ± 0.2	11	53
39	4-methylsulfonylphenyl	0.94	<6.0	>1000	4	20

[a] AlogP was calculated with Pipeline Pilot (Accelrys, Inc.; San Diego, CA, U.S.). [b] Displacement of specific [^{3}H]*N*-methyllysergic acid diethylamide ([^{3}H]LSD) binding in CHO cells stably expressing human 5-HT_6 receptor, expressed as K_i ± SEM (nM). [c] Luminescence measurement from a CHO-human-5-HT_6-aequorin assay, expressed as pA_2 ± SEM. [d] In vitro intrinsic clearance from hepatocyte assay [(μL/min)/10^6 cells].

Scheme 5. Synthesis of R^8 Arylsulfonyl Analogues via Two Approaches[a]

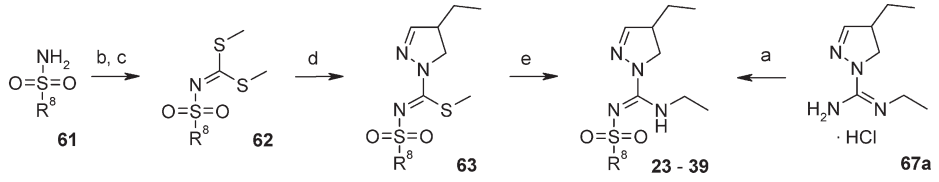

61d / 62d / 63ad: R^8 = 4-Cl-Ph
61e / 62e / 63ae: R^8 = 3-F-Ph
61f / 62f / 63af: R^8 = 3-CF_3-Ph
61g / 62g / 63ag: R^8 = 3,4-diCl-Ph
61h / 62h / 63ah: R^8 = 1-naphtyl
61i / 62i / 63ai: R^8 = 2-naphtyl
61j / 62j / 63aj: R^8 = 5-chloro-3-methylbenzo[b]thiophen-2-yl
61k / 62k / 63ak: R^8 = 6-chloroimidazo[2,1-b]thiazol-5-yl

[a] Reagents and conditions: (a) (i) R^8-SO_2Cl, DiPEA, DCM, room temp; (ii) 2 M aqueous NaOH extraction; (iii) SCX purification; (b) CS_2, KOH or NaOH, DMF/H_2O, 10 °C; (c) MeI, 10 °C to room temp; (d) **60a**, pyridine, reflux; (e) $EtNH_2$ [**64**, R^6 = Et, R^7 = H], MeOH, room temp.

structure even more vulnerable to metabolism. Despite being a predicted weak spot, substitution of the 5-position in **6** did not improve metabolic stability, as evidenced by **29**. On an R^8 phenyl substituent carrying two hydrophobic substituents, a 2,3- or 3,4-disubstitution pattern seemed most favorable for 5-HT_6R affinity (**32**, **33**, **34**), but this did not lead to the desired increase in metabolic stability. Strong negative effects on activity were seen when (di)substitution close to the sulfonyl linker forced the (hetero)aryl ring in distinct conformations (**30**, **31**, and **38**). Monocyclic heteroaryl groups with properly positioned substituents are well tolerated, exemplified by the less lipophilic analogue **37** (AlogP = 1.66). Although human metabolic stability of the latter increased relative to **6**, it actually decreased in rat, which would imply a serious limitation for preclinical research. The 4-methylsulfonylphenyl substituent in **39** relinquished 5-HT_6R activity altogether, indicated to be due to steric hindrance in the pocket by docking. Notably, this even more hydrophilic analogue (AlogP = 0.94) is the only compound demonstrating

dx.doi.org/10.1021/jm200466r |*J. Med. Chem.* 2011, 54, 7030–7054

Table 4. In Vitro Pharmacological Results of the Pyrazoline C4 SAR and Metabolic Stability Studies

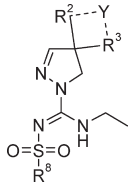

compd	R^2	R^3	R^8	AlogP [a]	K_i (5-HT$_6$), [b] nM	pA_2 (5-HT$_6$), [c]	Cl_{int}, human, [d]	Cl_{int}, rat, [d]
6 racemate	C_2H_5	H	3-Cl-Ph	2.73	7.9 ± 4.1	8.3 ± 0.1	53	92
40 (+)-enantiomer	C_2H_5	H	3-Cl-Ph	2.73	2.8 ± 0.5	8.0 ± 0.2	59	107
41 (−)-enantiomer	C_2H_5	H	3-Cl-Ph	2.73	16.4 ± 3.8	7.5 ± 0.2	49	126
42	CH_3	CH_3	3-Cl-Ph	2.69	24.1 ± 5.2	7.8 ± 0.1	14	77
43	C_2H_5	C_2H_5	3-Cl-Ph	2.95	49.9 ± 26.5	7.0 ± 0.2	34	116
44	$(CH_2)_4$		3-Cl-Ph	2.58	6.4 ± 3.1	8.2 ± 0.03	26	116
45	$(CH_2)_5$		3-Cl-Ph	3.68	5.2 ± 3.6	8.4 ± 0.3	48	139
46	$(CH_2)_2O(CH_2)_2$		3-Cl-Ph	1.92	71.1 ± 14.9	8.0 ± 0.4	5	82
47	$(CH_2)_2NH(CH_2)_2$		3-Cl-Ph	1.00	7.2 ± 0.7	8.7 ± 0.1	3	25
48	CH_2F	CH_2F	3-Cl-Ph	1.74	92.0 ± 22.2	<6.0	11	63
49	CH_3	CH_3	Ph	2.02	146.6 ± 42.8	7.2 ± 0.2	1	41

[a] AlogP was calculated with Pipeline Pilot (Accelrys, Inc.; San Diego, CA, U.S.). [b] Displacement of specific [^{3}H]*N*-methyllysergic acid diethylamide ([^{3}H]LSD) binding in CHO cells stably expressing human 5-HT$_6$ receptor, expressed as K_i ± SEM (nM). [c] Luminescence measurement from a CHO-human-5-HT$_6$-aequorin assay, expressed as pA_2 ± SEM. [d] In vitro intrinsic clearance from hepatocyte assay [(μL/min)/10^6 cells].

significantly lowered intrinsic clearance in both human and rat hepatocytes. Finally, the competitor-derived bicyclic heteroaromatic arylsulfonyl substituents in **35** (rise of AlogP to 4.20 and PSA to 110 Å^2) and **36** (more attractive AlogP of 1.95) gave activities similar to that of the lead structure. The latter showed improved human metabolic stability but somewhat lower rat metabolic stability. Another drawback of **36** was its affinity for the P-gp transporter (P-gp factor of 1.8), which is absent for other active compounds in Table 3. Moreover, its high calculated molecular polar surface area (PSA) of 128 Å^2 (vs 82 Å^2 for **6**) would not be beneficial either for CNS availability.[69]

In conclusion, none of the compounds evaluated resulted in an improved overall profile compared to **6** in terms of 5-HT$_6$R affinity and activity, metabolic stability, and molecular properties. Especially improvements in rat metabolic stability appeared to be challenging for this compound class. Attempts to tackle the metabolic issue were therefore reverted to variations at the pyrazoline ring.

Lead Optimization: Pyrazoline 4-Substitutions. As supported by modeling efforts, chiral separation of the racemic lead **6** showed that indeed both enantiomers are active on the 5-HT$_6$R, albeit with a moderate preference for the isomer with (+) optical rotation **40**. No significant difference was seen in intrinsic clearance of the (+)-enantiomer **40** and the (−)-enantiomer **41**. However, disubstitution of the pyrazoline C4 position would address the predicted weak spot on that position and seemed a viable opportunity given the lack of clear preference for any of the two enantiomers. As docking studies indicated that larger substituents at the pyrazoline C4-position may also be accommodated, di- and spiro-substituted analogues were synthesized, preferably with symmetrical substitution to obtain achiral compounds (Table 4).

Synthesis of the required 4,4-disubstituted pyrazoline building blocks required another strategy, since ring closure of α,β-unsaturated aldehydes or ketones with hydrazine (as set out in Scheme 1) limits the number of C4 substituents to one group R^2. We chose for base-assisted alkylation of malononitrile (**69**): for the acyclic disubstituted compounds two subsequent cycles of deprotonation followed by attack onto R^2-X or R^3-X (X = leaving group), and for the anticipated spiro analogues reaction with a linear molecule X-R^2-Y-R^3-X bearing a leaving group X at both termini in the presence of 2 equiv of base.[70,71] The nitrile groups of the formed dialkylated malononitriles **70** were fully reduced to the corresponding diamines **71** using $LiAlH_4$[72] or BH_3.[73] Oxidative ring closure of the diamines[74] furnished the 4,4-disubstituted 4,5-dihydro-3*H*-pyrazoles **72** (double bond between both nitrogens), which can tautomerize to the thermodynamically more stable 4,4-disubstituted 4,5-dihydro-1*H*-pyrazoles **73** (double bond between N2 and C3) under subsequent reaction conditions (or upon prolonged storage) to be incorporated into the target molecules according to the previously described routes through either intermediate **74** or **75** (Scheme 6).

For the only basic compound from this series, **47**, the nitrogen atom ending up in the spiro piperidyl ring was protected with a benzyl group throughout the whole synthesis and deprotected with 1-chloroethyl chloroformate (ACE-Cl) in the final step (to prevent concomitant reduction of the chloro substituent on the phenylsulfonyl moiety, which would take place upon catalytic hydrogenation). The symmetrical diamine intermediate **71g**, used to synthesize the pyrazoline **72g** incorporated in compound **48** (R^2 = R^3 = CH_2F), was unknown in literature to the best of our knowledge and could not be prepared via the dialkylation strategy described above. It was obtained via an alternative, seven-step procedure that is fully described in the Supporting Information.

With a highly similar AlogP, the achiral 4,4-dimethyl substituted pyrazoline analogue **42** showed a significant improvement in human metabolic stability compared to the 4-monoethyl substituted lead **6**, although rat metabolic stability only improved slightly. Less optimal filling of the hypothesized hydrophobic binding pocket (formed when D106 adopts the gauche$^+$ conformation) is a likely explanation for its somewhat reduced

Scheme 6. Synthesis of 4,4-Disubstituted Pyrazoline Analogues[a]

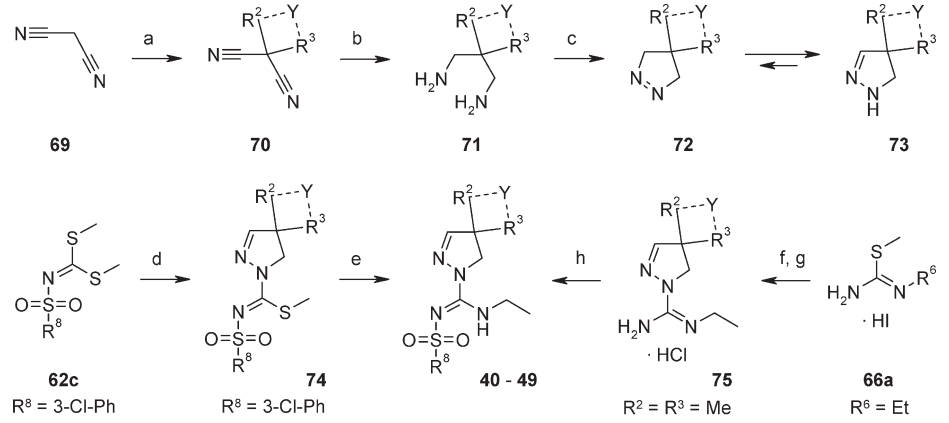

70 - 74: **a**: $R^2 = R^3 = Me$
b: $R^2 = R^3 = Et$
c: R^2-Y-R^3 = -$(CH_2)_4$-
d: R^2-Y-R^3 = -$(CH_2)_5$-
e: R^2-Y-R^3 = -$(CH_2)_2$-O-$(CH_2)_2$-
f: R^2-Y-R^3 = -$(CH_2)_2$-N(Bn)-$(CH_2)_2$-
71 - 74: **g**: $R^2 = R^3 = CH_2F$

[a] Reagents and conditions: (a) R^2-X + R^3-X or X-R^2-Y-R^3-X, KO-*t*-Bu, TBAB, DMSO (optional), 0 °C to room temp or DBU, DMF, 0 to 80 °C or K_2CO_3, DMF, 65 °C [X = halogen]; (b) $LiAlH_4$, Et_2O or CPME, 0 °C to room temp or BH_3·THF, THF, −10 to 60 °C; (c) NaClO, H_2O_2, MeOH/H_2O, 0 °C to room temp; (d) **72**, pyridine, reflux; (e) $EtNH_2$, MeOH, room temp; (f) **72a**, pyridine, reflux; (g) HCl, *i*-PrOH/EtOAc; (h) R^8-SO_2Cl, DiPEA, DCM, room temp [R^8 = Ph].

5-HT_6R affinity. When going to the 4,4-diethyl substituted analogue **43** (slight rise of AlogP to 2.95), some of the gain in human metabolic stability (and all in rat) was lost but also the affinity showed a drop rather than the anticipated gain. However, by rigidification of its substituents into spiro five-membered ring analogue **44** (AlogP = 2.58), apparently a more optimal fit in the hydrophobic pocket was achieved given the clear improvement in measured K_i and pA_2 values. Human metabolic stability was still better than that of lead **6**, whereas rat metabolic stability was already somewhat negatively affected. Growing the size of the hydrophobic spiro substituent to a six-membered ring in **45** (significant rise of AlogP to 3.68) further improved 5-HT_6R affinity but again at the cost of metabolic stability, ending with similar human and higher rat intrinsic clearance compared to lead **6**. By introduction of an oxygen atom in the ring (**46**, AlogP = 1.92), a reduced metabolic rate was observed that was more pronounced in human than in rat hepatocytes. The lowered hydrophobicity of the spiro ring likely contributes to this but at the same time results in a clear reduction in 5-HT_6R affinity. The heteroatom variation made in **47** (AlogP = 1.00, PSA = 94 $Å^2$) was primarily aimed at confirming our hypotheses and supporting the followed strategy. This analogue is the only one with a basic residue, according to docking studies, well-posed for interaction with D106 when changed into the trans conformation (Figure 3D). This is the same interaction observed for "classical" 5-HT_6R ligands containing a positive charge, such as **50** (Figure 3C). As expected **47** shows favorable receptor binding and functional activity data, although the gain compared to **45** is marginal. Whereas a salt bridge with **47** should give a stronger enthalpy gain than the hydrophobic interaction with **45**, a desolvation penalty for the more polar **47** will likely in part counterbalance this difference. Again, it is seen that the presence of a heteroatom in the spiro ring is clearly beneficial for metabolic stability, in this case also with a marked improvement in rat.

Although the foregoing makes **47** appear an ideal optimized lead, off-target selectivity was a concern. Profiling in a panel of 118 receptor, ion channel, and transporter assays and 42 enzyme assays at Cerep[60] showed, contrary to nonbasic lead structure **6**, some affinity toward other monoaminergic GPCRs. Nonetheless, with pK_i between 5.0 and 6.1 measured in the 5-HT_{2A}, 5-HT_{2B}, 5-HT_3, M_1, M_3, M_4, M_5, and nonselective σ receptor binding assays, a relatively large window to 5-HT_6R affinity still exists (see Supporting Information for full data). Membrane passage of **47** was, with 14.7%, lower than that of **6** but not critical. However, a clear increase in P-gp affinity was seen (P-gp factor of 18.9). Even more important, screening of **47** on hERG confirmed that a basic nitrogen in this class contributes to affinity for this antitarget. Although the hERG affinity was relatively low (pIC_{50} of 5.1 (Zenas)[59]), the low plasma protein binding of this compound (66% in human and 59% in rat (Cyprotex)[75]) likely accounted for sufficient peripheral exposure of free **47** to cause prolongation of the QT interval of 25 ms at a dose of 50 mg/kg per os (po) in our telemetered conscious freely moving guinea pig QTc model.[76] No significant QTc effect was seen at a lower dose of 10 mg/kg po.

As such we reverted to compound **42**, providing the best compromise between 5-HT_6R affinity and functional activity, human and rat metabolic stability, CNS druglike properties, and off-target selectivity. Two final modifications of this compound were made to complete our SAR picture. With an apparent tendency for metabolism in the alkyl groups on the pyrazoline C4 position, we investigated whether introduction of a fluoro substituent on both methyl groups in **42** would lead to a lower intrinsic clearance. Regretfully, analogue **48** (AlogP = 1.74) only showed a marginal gain in both human and rat metabolic stability, whereas receptor binding and functional activity were seriously affected. Removal of the 3-chloro substituent in **42** to get to analogue **49** (AlogP = 2.02), bearing the unsubstituted

dx.doi.org/10.1021/jm200466r |*J. Med. Chem.* 2011, 54, 7030–7054

phenylsulfonyl residue as in **50**, resulted in a clear improvement in metabolic stability. However, in line with the proposed polar interaction of the 3-chloro substituent with Q291, the 5-HT_6R affinity of **49** is significantly reduced compared to **42**, rendering it uninteresting from a pharmacological point of view.

Profiling of Compound 42. On the basis of the necessary trade-off between potency and metabolic stability emerging from the lead optimization efforts described, achiral compound **42** was considered to be an appropriate frontrunner candidate. With a molecular weight of 343, an AlogP of 2.69, a PSA of 82 $Å^2$, one H-bond donor, six H-bond acceptors, and five rotational bonds, its calculated molecular properties are CNS druglike. Membrane passage is excellent (41%), and it has no affinity for the P-gp transporter (P-gp factor of 1.0). When profiled comprehensively at Cerep[60] in a panel of 86 receptor, ion channel, and transporter assays and 27 enzyme assays, the only off-target affinities measured were a pK_i of 5.8 for the peripheral benzodiazepine receptor and a pK_i of 5.1 for the 5-HT_{2B} receptor (see Supporting Information for full data). Significant CYP inhibition was not observed, with $pIC_{50} < 5$ measured for all CYPs tested (1A2, 2C9, 2C19, 2D6, and 3A4). Most importantly, **42** is devoid of a basic moiety and was shown to be free of hERG affinity ($pIC_{50} < 5$ with a PI of 15 at 10^{-5} M measured at Zenas[59]). Despite a high free fraction in plasma (plasma protein binding 63% measured at Cyprotex[75]), the compound was confirmed to be free of QTc effects at doses up to 100 mg/kg sc in guinea pig.[76] On the basis of in vitro intrinsic clearance in hepatocytes, human metabolic stability appears to be acceptable whereas it is suboptimal in rat. The latter is reflected by the rat in vivo pharmacokinetic (PK) results. Absorption was very fast (t_{max} = 0.5 h), likely aided by the nonionizable character of the molecule and the high membrane permeability. Oral bioavailability in rat was low (~7%), which was clearly confirmed to be due to a high first-pass effect in an accelerated infusion study (significantly higher exposures in the intravenous (iv) curve compared to the nearly parallel intraduodenal (id) and intravenoportal (ivp) curves; data not shown). However, with intraperitoneal (ip) administration a rat bioavailability of 45% could be achieved. Calculation of the clearance after iv administration indicated it to be at the liver blood flow. A plasma half-life of just under 2 h was determined both after iv and po administration. With a CNS/plasma ratio of 1.0, the compound was shown to be brain-penetrable, and the relatively high in vitro fraction unbound in brain homogenate[77] of 0.10 will contribute to sufficient exposure of free drug in the brain. Altogether, this rat PK/PD profile was considered good enough to investigate **42** as a frontrunner from this unique structural class in rat in vivo models predicted to be relevant for indications associated with the 5-HT_6R. A study to compare the potential of **42**, **47**, and **50** to improve scopolamine-induced deficits in rat models for episodic memory is published elsewhere.[78]

CONCLUSIONS

A broad scope of medicinal chemistry tools have enabled us to gain proper knowledge of molecular properties and target−ligand interactions of a unique, nonbasic structural class of 5-HT_6R antagonists identified by HTS hit **1** and explored with hit-to-lead analogues **2**−**15**. This has allowed us to efficiently narrow the large diversity possible around the identified core structure **58** and to design lead optimization programs around distinct substituents in order to improve 5-HT_6R potency and/or metabolic stability while trying to keep the molecules CNS druglike. The absence of a basic nitrogen, in all target compounds **1**−**49** except **47**, contributed to exceptional selectivity toward off-targets (like other monoaminergic GPCRs) and antitargets (like hERG). This may be especially beneficial in envisaged scenarios where 5-HT_6R antagonists will be developed as adjunctive therapies. In this class of nonbasic *N*′-(arylsulfonyl)pyrazoline-1-carboxamidines, the absence of a salt bridge interaction with the receptor is compensated by a combination of two factors. First, there is a favorable entropy contribution due to an internal hydrogen bond that stabilizes the bioactive conformation. Second, an enthalpy gain is possible due to hydrophobic interactions with a pocket that becomes available when, in the absence of a protonated basic interaction partner, D106 changes conformation to interact with Y310 in the receptor. During the phases of lead optimization described here, we came across an apparent trade-off between potency and metabolic stability while varying different parts of the structure. While we were sometimes successful in improving human in vitro intrinsic clearance, it proved to be particularly challenging to significantly improve rat metabolic stability, especially when simultaneously trying to keep other properties compliant with CNS druglike criteria. A compound within this series featuring a well-suited overall balance was **42**. Being profiled as potent, selective, hERG-free, and CNS available, it appears to be a suitable candidate for further in vivo pharmacological testing. On the basis of in vitro intrinsic clearance data obtained from hepatocytes, predictions for the human PK profile are more favorable than for rat.

EXPERIMENTAL SECTION

Chemistry. Unless stated otherwise, starting materials, reagents and solvents were purchased as high-grade commercial products and were used without further purification. Reactions sensitive to moisture and/or oxygen were carried out under an inert atmosphere of anhydrous nitrogen, with solvents dried by the Pure-Solv EN solvent purification system (Innovative Technology, Inc.). Yields refer to isolated pure products and were not maximized.

Analytical thin-layer chromatography (TLC) was performed on Merck precoated 60 F_{254} plates, and spots were visualized with UV light (254 nm), I_2, 10% phosphomolybdic acid solution in ethanol, ninhydrin solution, permanganate solution, anisaldehyde solution, bromocresol green solution, or 2,4-dinitrophenylhydrazine solution. Flash chromatography was performed on glass column using silica gel 60 (0.040−0.063 mm, Merck) or on a Büchi Sepacore automated flash system equipped with a Supelco VersaFlash station employing Supelco VersaPak silica cartridges. Column chromatography was performed using silica gel 60 (0.063−0.200 mm, Merck).

^1H and ^{13}C nuclear magnetic resonance (NMR) spectra were recorded using the standard methods provided by the manufacturer at room temperature, unless indicated otherwise, on a Bruker Avance 400 instrument (^1H, 400 MHz), a Varian UN400 instrument (^1H, 400 MHz), or a Varian VXR200 instrument (^1H, 200 MHz) in the indicated deuterated solvent (i.e., DMSO-d_6 or $CDCl_3$) with tetramethylsilane as an internal standard. Chemical shifts (δ scale) are given in parts per million (ppm) downfield from tetramethylsilane. Coupling constants (J) are expressed in hertz (Hz). The following abbreviations are used to describe peak patterns: s (singlet), d (doublet), dd (double doublet), ddd (double double doublet), t (triplet), dt (double triplet), q (quartet), dq (double quartet), m (multiplet) and br (broad).

Melting points were recorded on a Büchi B-545 melting point apparatus and are uncorrected.

Mass spectra were recorded on a Micromass QTOF-2 (quadrupole time-of-flight) instrument with MassLynx application software for

Table 5[a]

step	total time (min)	flow (μL/min)	solvent A (%)	solvent B (%)
0	0	2000	95	5
1	1.8	2000	0	100
2	2.5	2000	0	100
3	2.7	2000	95	5
4	3.0	2000	95	5

[a] A = 100% water with 0.1% HCOOH, pH ≈ 3. B = 100% acetonitrile with 0.1% HCOOH.

Table 6[a]

step	total time (min)	flow (μL/min)	solvent A (%)	solvent B (%)
0	0.2	1600	90	10
1	2.5	1600	0	100
2	2.8	1600	0	100
3	2.9	1600	90	10
4	3.10	1600	90	10
5	3.11	500	90	10

[a] A = 100% water with 0.2% HCOOH. B = 100% acetonitrile with 0.2% HCOOH.

acquisition and reconstruction of the data. Exact mass measurement by HRMS was done of the quasimolecular ion $[M + H]^+$.

Optical rotations ($[\alpha]_D$) were measured on an Optical Activity polarimeter. Specific rotations are given as deg/dm, and the concentrations are reported as g/100 mL of the specified solvent and were recorded at 23 °C.

Spectroscopic data of all described compounds were consistent with the proposed structures. The purity of the target compounds **1**−**49** was established as ≥95%, based on liquid chromatography−mass spectrometry (LC−MS) analysis (average from ultraviolet (UV) detection and evaporative light scattering detector (ELSD)) by one of the two systems described below, except for **35** (94%), **36** (92%), and **38** (94%).

The first LC−MS system consisted of two Perkin-Elmer series 200 micropumps connected to each other by a 50 μL tee mixer, with a Gilson 215 autosampler connected. The autosampler had a 2 μL injection loop and was connected to a Waters Atlantis C18 30 mm × 4.6 mm column with 3 μm particles, thermostated in a Perkin-Elmer series 200 column oven at 40 °C. The column was connected to a Perkin-Elmer series 200 UV meter with a 2.7 μL flow cell. The wavelength was set to 254 nm. The UV meter was connected to a Sciex API 150EX mass spectrometer with the following parameters: scan range, 150−900 amu; polarity, positive; scan mode, profile; resolution Q1, UNIT; step size, 0.10 amu; time per scan, 0.500 s; NEB, 10; CUR, 10; IS, 5200; TEM, 325; DF, 30; FP, 225; EP, 10. The evaporative light scattering detector was a Sedere Sedex 55 operating at 50 °C and 3 bar of N_2, connected to the Sciex API 150. The complete system was controlled by a G3 Power Mac. Table 5 shows the gradient elution method used as a standard.

The second LC−MS system consisted of Waters 1525μ pumps, connected to a Waters 2777 autosampler. The autosampler had a 10 μL injection loop, and the injection volume was 10 μL. The autosampler was connected to a Waters Sunfire C18 30 mm × 4.6 mm column with 2.5 μm particles, thermostated at 23 °C. The column was connected to a Waters 2996 PDA, and the wavelength was scanned from 240 to 320 nm with 1.2 nm resolution and 20 Hz sampling rate. After the PDA the flow was split 1:1 and connected to a Waters 2424 ELSD and a Waters ZQ mass detector. The ELSD operated with the following parameters: gas pressure, 40 psi; data rate, 20 points/s; gain, 500; time constant, 0.2 s; nebulizer mode, cooling; drift tube, 50 °C. The mass spectrometer operated with the following parameters: scan range, 117−900 amu; polarity, positive; data format, centroid; time per scan, 0.500 s; interscan time, 0.05 s; capillary, 2.5 kV; cone, 25 V; extractor, 2 V; RF lens, 0.5 V; source temp, 125 °C; desolvation temp, 400 °C; cone gas, 100 L/h; desolvation gas, 800 L/h; LM 1 resolution, 15; HM 1 resolution, 15; ion energy, 0.5; multiplier, 500 V. The complete system was controlled by Masslynx 4.1. Table 6 shows the gradient elution method used as a standard.

Syntheses. *N*′-(2-Chlorophenylsulfonyl)-*N*,4-diethyl-4,5-dihydro-1*H*-pyrazole-1-carboxamidine (1). **63aa** (1.30 g, 3.76 mmol) was dissolved in 10 mL of MeOH. A 70% solution of ethylamine in water (5 mL, excess) was added, and the mixture was stirred for 1 h at room temperature. The mixture was concentrated under reduced pressure and the crude product was purified by flash chromatography (Et_2O) to give 1.09 g (85%) of **1** as a colorless oil. ^{1}H NMR (400 MHz, $CDCl_3$) δ 0.96 (t, *J* = 7.5 Hz, 3H), 1.16 (t, *J* = 7.3 Hz, 3H), 1.41−1.70 (m, 2H), 3.03−3.17 (m, 1H), 3.44−3.58 (m, 2H), 3.71 (dd, *J* = 11.4 and 7.5 Hz, 1H), 4.11 (t, *J* = 11.2 Hz, 1H), 6.90 (br s, 1H), 6.93 (d, *J* = 1.5 Hz, 1H), 7.30−7.40 (m, 2H), 7.45 (dd, *J* = 7.8 and 1.6 Hz, 1H), 8.15 (dd, *J* = 7.6 and 2.0 Hz, 1H).

N′-(2-Chlorophenylsulfonyl)-*N*-benzyl-4-ethyl-4,5-dihydro-1*H*-pyrazole-1-carboxamidine (2). Following the same procedure as described for **1**, reaction of **63aa** (700 mg, 2.02 mmol) with benzylamine (3 mL, excess) and purification by flash chromatography (Et_2O) gave 700 mg (85%) of **2** as a colorless oil. ^{1}H NMR (400 MHz, $CDCl_3$) δ 0.96 (t, *J* = 7.4 Hz, 3H), 1.45−1.68 (m, 2H), 3.07−3.20 (m, 1H), 3.79 (dd, *J* = 10.7 and 7.7 Hz, 1H), 4.21 (t, *J* = 10.7 Hz, 1H), 4.64 (d, *J* = 5.5 Hz, 2H), 6.93 (d, *J* = 1.6 Hz, 1H), 7.07 (br s, 1H), 7.20−7.31 (m, 5H), 7.33 (dd, *J* = 7.4 and 1.3 Hz, 1H), 7.39 (td, *J* = 7.6 and 1.7 Hz, 1H), 7.46 (dd, *J* = 7.8 and 1.4 Hz, 1H), 8.14 (dd, *J* = 7.9 and 1.8 Hz, 1H).

N′-(2-Chlorophenylsulfonyl)-*N*-phenyl-4-ethyl-4,5-dihydro-1*H*-pyrazole-1-carboxamidine (3). **63aa** (1.00 g, 2.89 mmol) and aniline (0.26 mL, 2.89 mmol) were dissolved in 10 mL of dry tetrahydrofuran (THF), and the solution was cooled in an ice bath. Subsequently, 3.18 mL of a 1 M solution of NaHMDS in THF was added dropwise, and stirring was continued for 20 min at room temperature. The mixture was concentrated under reduced pressure. Water was added, and the mixture was extracted twice with EtOAc. The combined organic layers were dried over Na_2SO_4, filtered, and concentrated under reduced pressure. The crude product was purified by flash chromatography (gradient Et_2O/petroleum ether (PE) = 1:1 to Et_2O). The residue was triturated with diisopropyl ether, filtered off, and dried in vacuo to give 180 mg (16%) of **3** as white crystals, mp 128−130 °C. ^{1}H NMR (400 MHz, $CDCl_3$) δ 0.97 (t, *J* = 7.4 Hz, 3H), 1.45−1.69 (m, 3H), 3.07−3.19 (m, 1H), 3.82 (dd, *J* = 11.8 and 7.2 Hz, 1H), 4.21 (t, *J* = 11.3 Hz, 1H), 6.87 (d, *J* = 1.6 Hz, 1H), 7.01 (d, *J* = 7.7 Hz, 2H), 7.05−7.11 (m, 1H), 7.19 (t, *J* = 7.7 Hz, 2H), 7.31 (td, *J* = 7.8, 7.3, and 1.5 Hz, 1H), 7.40 (td, *J* = 7.6 and 1.8 Hz, 1H), 7.45 (dd, *J* = 8.0 and 1.4 Hz, 1H), 8.12 (dd, *J* = 7.8 and 1.7 Hz, 1H), 8.68 (br s, 1H).

N′-(2-Chlorophenylsulfonyl)-*N*-isopropyl-4-ethyl-4,5-dihydro-1*H*-pyrazole-1-carboxamidine (4). Following the same procedure as described for **1**, reaction of **63aa** (700 mg, 2.02 mmol) with isopropylamine (3 mL, excess) and purification by flash chromatography (Et_2O) gave 620 mg (86%) of **4** as a pale yellow oil. ^{1}H NMR (400 MHz, $CDCl_3$) δ 0.95 (t, *J* = 7.5 Hz, 3H), 1.11 (d, *J* = 6.5 Hz, 3H), 1.12 (d, *J* = 6.5 Hz, 3H), 1.43−1.68 (m, 2H), 3.09 (m, 1H), 3.75 (dd, *J* = 11.4 and 7.5 Hz, 1H), 4.19 (m, 2H), 5.23 (br s, 1H), 6.92 (d, *J* = 1.5 Hz, 1H), 7.33 (td, *J* = 7.7 and 1.8 Hz, 1H), 7.38 (td, *J* = 7.6 and 1.8 Hz, 1H), 7.47 (dd, *J* = 7.7 and 1.8 Hz,1H), 8.15 (dd, *J* = 7.7 and 1.8 Hz, 1H).

N′-(Phenylsulfonyl)-*N*,4-diethyl-4,5-dihydro-1*H*-pyrazole-1-carboxamidine (5). Following the same procedure as described for **1**, reaction of **63ab** (2.99 g crude, max 8.63 mmol) with ethylamine (5 mL of a 70% solution in water, excess) and purification by flash chromatography (Et_2O) followed by crystallization from methyl *tert*-butyl

ether (MtBE) gave 1.66 g (53% over two steps) of **5** as white crystals, mp 43−45 °C. ^{1}H NMR (400 MHz, $CDCl_3$) δ 0.94 (t, J = 7.4 Hz, 3H), 1.12 (t, J = 7.3 Hz, 3H), 1.41−1.67 (m, 2H), 3.00−3.14 (m, 1H), 3.40−3.51 (m, 2H), 3.68 (dd, J = 11.4 and 7.4 Hz, 1H), 4.07 (t, J = 11.7 Hz, 1H), 6.86 (br s, 1H), 6.89 (d, J = 1.6 Hz, 1H), 7.35 (br s, 1H), 7.39 (t, J = 7.8 Hz, 1H), 7.38−7.48 (m, 3H), 7.89−7.95 (m, 2H).

***N′*-(3-Chlorophenylsulfonyl)-*N*,4-diethyl-4,5-dihydro-1*H*-pyrazole-1-carboxamidine (6).** Following the same procedure as described for **1**, reaction of **63ac** (700 mg, 2.02 mmol) with ethylamine (3 mL of a 70% solution in water, excess) gave 670 mg (97%) of **6** as a pale yellow oil. ^{1}H NMR (400 MHz, $CDCl_3$) δ 0.95 (t, J = 7.4 Hz, 3H), 1.14 (t, J = 7.2 Hz, 3H), 1.43−1.67 (m, 2H), 3.04−3.17 (m, 1H), 3.40−3.51 (m, 2H), 3.68 (dd, J = 11.5 and 7.4 Hz, 1H), 4.08 (t, J = 11.3 Hz, 1H), 6.79 (br s, 1H), 6.92 (d, J = 1.6 Hz, 1H), 7.37 (t, J = 7.9 Hz, 1H), 7.42 (ddd, J = 8.0, 2.0, and 1.3 Hz, 1H), 7.80 (dt, J = 7.6 and 1.4 Hz, 1H), 7.91 (t, J = 1.8 Hz, 1H).

***N′*-(3-Chlorophenylsulfonyl)-*N*-propyl-4-ethyl-4,5-dihydro-1*H*-pyrazole-1-carboxamidine (7).** Following the same procedure as described for **1**, reaction of **63ac** (423 mg, 1.22 mmol) with propylamine (1.0 mL, 12.20 mmol) and purification by flash chromatography (dichloromethane (DCM)) gave 430 mg (99%) of **7** as a colorless oil. ^{1}H NMR (400 MHz, $CDCl_3$) δ 0.90 (t, J = 7.4 Hz, 3H), 0.98 (t, J = 7.4 Hz, 3H), 1.47−1.69 (m, 4H), 3.07−3.19 (m, 1H), 3.39 (q, J = 6.4 Hz, 2H), 3.72 (dd, J = 11.1 and 7.3 Hz, 1H), 4.12 (t, J = 11.1 Hz, 1H), 6.85 (br s, 1H), 6.94 (d, J = 1.5 Hz, 1H), 7.39 (t, J = 7.9 Hz, 1H), 7.43−7.46 (m, 1H), 7.81−7.85 (m, 1H), 7.94 (t, J = 1.8 Hz, 1H).

***N′*-(3-Chlorophenylsulfonyl)-*N*-methyl-4-ethyl-4,5-dihydro-1*H*-pyrazole-1-carboxamidine (8).** Following the same procedure as described for **1**, reaction of **63ac** (500 mg, 1.45 mmol) with methylamine hydrochloride (976 mg, 14.45 mmol) in the presence of triethylamine (2.4 mL, 17.35 mmol) and purification by flash chromatography (DCM) gave 470 mg (99%) of **8** as a colorless oil. ^{1}H NMR (400 MHz, $CDCl_3$) δ 0.97 (t, J = 7.7 Hz, 3H), 1.47−1.69 (m, 2H), 3.04 (d, J = 5.1 Hz, 1H), 3.08−3.19 (m, 1H), 3.71 (dd, J = 11.1 and 7.3 Hz, 1H), 4.11 (t, J = 11.1 Hz, 1H), 6.88 (br s, 1H), 6.94 (d, J = 1.1 Hz, 1H), 7.39 (t, J = 7.9 Hz, 1H), 7.43−7.47 (m, 1H), 7.81−7.86 (m, 1H), 7.95 (t, J = 1.8 Hz, 1H).

***N′*-(3-Chlorophenylsulfonyl)-4-ethyl-4,5-dihydro-1*H*-pyrazole-1-carboxamidine (9).** Following the same procedure as described for **1**, reaction of **63ac** (300 mg, 0.87 mmol) with ammonia (excess, bubbled through the reaction mixture) and purification by trituration with Et_2O followed by filtration and drying in vacuo gave 220 mg (81%) of **9** as white crystals, mp 140.5−141.7 °C. ^{1}H NMR (400 MHz, $CDCl_3$) δ 0.97 (t, J = 7.7 Hz, 3H), 1.45−1.68 (m, 2H), 3.13−3.18 (m, 1H), 3.54 (dd, J = 11.4 and 7.4 Hz, 1H), 3.93 (t, J = 11.7 Hz, 1H), 6.23 (br s, 1H), 6.94 (d, J = 1.6 Hz, 1H), 7.35 (br s, 1H), 7.39 (t, J = 7.8 Hz, 1H), 7.45−7.48 (m, 1H), 7.80−7.85 (m, 1H), 7.92 (t, J = 1.8 Hz, 1H).

***N′*-(3-Chlorophenylsulfonyl)-*N*-ethyl-4-methyl-4,5-dihydro-1*H*-pyrazole-1-carboxamidine (10).** Following the same procedure as described for **1**, reaction of **63bc** (500 mg crude, max 1.50 mmol) with ethylamine (1 mL of a 70% solution in water, excess) and purification by flash chromatography (gradient Et_2O/PE = 1:1 to Et_2O) gave 410 mg (48% over two steps) of **10** as a colorless oil. ^{1}H NMR (400 MHz, $CDCl_3$) δ 1.16 (t, J = 7.0 Hz, 3H), 1.20 (d, J = 7.0 Hz, 3H), 3.16−3.30 (m, 1H), 3.41−3.52 (m, 2H), 3.62 (dd, J = 11.3 and 7.5 Hz, 1H), 4.17 (t, J = 11.3 Hz, 1H), 6.80 (br s, 1H), 6.89 (d, J = 1.5 Hz, 1H), 7.38 (dd, J = 7.7 and 7.6 Hz, 1H), 7.43 (ddd, J = 8.0, 2.0, and 1.2 Hz, 1H), 7.82 (ddd, J = 7.6, 1.8, and 1.3 Hz, 1H), 7.92 (t, J = 1.8 Hz, 1H).

***N′*-(3-Chlorophenylsulfonyl)-*N*-ethyl-4,5-dihydro-1*H*-pyrazole-1-carboxamidine (11).** Following the same procedure as described for **1**, reaction of **63cc** (500 mg, 1.57 mmol) with ethylamine (1 mL of a 70% solution in water, excess) and purification by flash chromatography (Et_2O) gave 400 mg (81%) of **11** as a colorless oil. ^{1}H NMR (400 MHz, $CDCl_3$) δ 1.16 (t, J = 7.2 Hz, 3H), 2.89 (t, J = 9.6 Hz, 1H), 3.42−3.51 (m, 2H), 3.71 (dd, J = 11.4 and 7.4 Hz, 1H), 4.01 (t, J = 10.0 Hz, 1H), 6.82 (br s, 1H), 7.02 (t, J = 1.7 Hz, 1H), 7.38 (t, J = 7.9 Hz, 1H), 7.43 (ddd, J = 8.0, 1.9, and 1.2 Hz, 1H), 7.81 (ddd, J = 7.6, 1.5, and 1.4 Hz, 1H), 7.92 (t, J = 1.7 Hz, 1H).

***N′*-(3-Chlorophenylsulfonyl)-*N*-ethyl-3-methyl-4,5-dihydro-1*H*-pyrazole-1-carboxamidine (12).** Following the same procedure as described for **1**, reaction of **63dc** (590 mg crude, max 1.78 mmol) with ethylamine (1 mL of a 70% solution in water, excess) and purification by flash chromatography (DCM/acetone = 98:2 to 95:5) gave 340 mg (22% over two steps) of **12** as a colorless oil. ^{1}H NMR (400 MHz, $CDCl_3$) δ 1.14 (t, J = 7.3 Hz, 3H), 2.04 (s, 3H), 2.82 (t, J = 9.8 Hz, 2H), 3.39−3.48 (m, 2H), 4.08 (t, J = 9.8 Hz, 2H), 6.65 (br s, 1H), 7.36 (t, J = 7.8 Hz, 1H), 7.40−7.44 (m, 1H), 7.79−7.83 (m, 1H), 7.92 (t, J = 1.8 Hz, 1H).

***N′*-(3-Chlorophenylsulfonyl)-*N*,*N*-dimethyl-4-ethyl-4,5-dihydro-1*H*-pyrazole-1-carboxamidine (13).** Following the same procedure as described for **1**, reaction of **63aa** (700 mg, 2.02 mmol) with dimethylamine (excess, bubbled through the reaction mixture) and purification by crystallization from MtBE gave 270 mg (39%) of **13** as white crystals, mp 94−95 °C. ^{1}H NMR (400 MHz, $CDCl_3$) δ 0.92 (t, J = 7.5 Hz, 3H), 1.41−1.63 (m, 2H), 2.93−3.06 (m, 1H), 3.15 (s, 6H), 3.52 (dd, J = 11.4 and 7.0 Hz, 1H), 3.90 (t, J = 11.0 Hz, 1H), 6.95 (d, J = 1.5 Hz, 1H), 7.30−7.40 (m, 2H), 7.45 (dd, J = 7.8 and 1.6 Hz, 1H), 8.18 (dd, J = 7.6 and 2.0 Hz, 1H).

***N′*-(3-Chlorophenylsulfonyl)-*N*-ethyl-5-phenyl-4,5-dihydro-1*H*-pyrazole-1-carboxamidine (14).** Following the same procedure as described for **1**, reaction of **63ec** (1.00 g, 2.54 mmol) with ethylamine (3 mL of a 70% solution in water, excess) and purification by crystallization from EtOH/water = 4:1 followed by drying in vacuo gave 700 mg (71%) of **14** as white crystals, mp 124−126 °C. ^{1}H NMR (400 MHz, $CDCl_3$) δ 1.21 (t, J = 7.1 Hz, 3H), 2.73 (ddd, J = 18.7, 6.6, and 1.8 Hz, 1H), 3.37 (ddd, J = 18.7, 11.8, and 1.7 Hz, 1H), 3.56−3.72 (m, 2H), 5.44 (dd, J = 11.8 and 6.6 Hz, 1H), 6.98 (br s, 1H), 6.99 (d, J = 1.5 Hz, 1H), 7.07 (t, J = 8.1 Hz, 1H), 7.19 (dd, J = 4.8 and 1.8 Hz, 1H), 7.28 (ddd, J = 7.9, 2.0, and 1.2 Hz, 1H), 7.39 (t, J = 1.8 Hz, 1H).

***N′*-(3-Chlorobenzoyl)-*N*,4-diethyl-4,5-dihydro-1*H*-pyrazole-1-carboxamidine (15).** **67a** (200 mg, 0.98 mmol) was suspended in 5 mL of DCM. Diisopropylethylamine (0.36 mL, 2.06 mmol) and 3-chlorobenzoyl chloride (154 mg, 0.88 mmol) were added, and the mixture was stirred overnight at room temperature. The mixture was washed with 5% aqueous $NaHCO_3$ followed by 2 M NaOH and the organic layer was dried over Na_2SO_4, filtered, and concentrated under reduced pressure to give 200 mg (74%) of **15** as a yellow oil. ^{1}H NMR (400 MHz, $CDCl_3$) δ 0.99 (t, J = 7.5 Hz, 3H), 1.24 (t, J = 7.2 Hz, 3H), 1.49−1.71 (m, 2H), 3.08−3.24 (m, 1H), 3.32−3.76 (m, 3H), 3.96−4.21 (m, 1H), 6.37 (br s, 1H), 6.93 (d, J = 1.5 Hz, 1H), 7.32 (t, J = 7.9 Hz, 1H), 7.38−7.42 (m, 1H), 8.03−8.06 (m, 1H), 8.16 (t, J = 1.8 Hz, 1H).

Compounds 16 and 17 from Chiral Separation of 14. The enantiomers of **14** were separated by chiral preparative HPLC. The chiral preparative HPLC system consisted of a 250 mm × 80 mm axial compression column packed with CHIRALCELOD as stationary phase and heptane/ethanol (80:20) as mobile phase. The flow rate used was 240 mL/min, and detection was done by using UV set at a wavelength of 230 nm. The racemate was injected as a solution of 4.5% m/v in heptane:/ethanol (40:60).

The first eluting enantiomer **16** was isolated in 89% yield with an ee of >99; $[\alpha]_D$ −37 (c 1, $CHCl_3$). ^{1}H NMR (400 MHz, $CDCl_3$) data were identical to the spectrum of the racemate (**14**).

The second eluting enantiomer **17** was isolated in 89% yield with an ee of >99; $[\alpha]_D$ +38 (c 1, $CHCl_3$). ^{1}H NMR (400 MHz, $CDCl_3$) data were identical to the spectrum of the racemate (**14**).

For both enantiomers, the amorphous materials obtained from evaporation of the chiral preparative HPLC mobile phase were crystallized from EtOH. Crystals of the (+)-enantiomer **17** were of suitable quality for determination of the absolute configuration by X-ray.

Selected Crystallographic Data for ***17***. X-ray data were collected at the Bijvoet Centre for Biomolecular Research, Utrecht University, The Netherlands, with a Nonius KappaCCD diffractometer on a rotating anode using Mo Kα radiation at 150 K. The structure was solved with the program SHELXS97 (G. M. Sheldrick) and refined with SHELXL97 (G. M. Sheldrick). The program PLATON[79] was used for the analysis of the geometry, the illustrations, and the validation of the results. Crystal system, monoclinic; space group, $P2_1$; unit cell dimensions, a = 8.8409 Å, b = 11.2526 Å, c = 9.25158 Å; overall R-factor, 0.0254. The CIF has been deposited at the Cambridge Crystallographic Data Centre (CCDC), deposition number 817440.

***N′*-(3-Chlorophenylsulfonyl)-*N*-ethyl-5-(pyridin-4-yl)-4,5-dihydro-1*H*-pyrazole-1-carboxamidine (18).** Following the same procedure as described for **1**, **63fc** (1.76 g crude, max 4.4 mmol) was reacted with ethylamine (2 mL of a 70% solution in water, excess). The crude product was purified by flash chromatography (DCM, DCM/MeOH = 99:1 to 96:4). Subsequently, the evaporation residue from the combined product fractions was dissolved in MeOH and brought onto a conditioned SCX ion exchange column, the column was washed with MeOH, and the product was eluted with 1 M NH_3 in MeOH. Evaporation yielded 680 mg (21% over two steps) of **18** as a beige solid. ^{1}H NMR (400 MHz, $CDCl_3$) δ 1.27 (t, J = 7 Hz, 3H), 2.62−2.72 (m, 1H), 3.33−3.45 (m, 1H), 3.60−3.79 (m, 2H), 5.34−5.45 (m, 1H), 6.88 (d, J = 6 Hz, 2H), 7.01(br s, 1H), 7.10−7.22 (m, 2H), 7.35 (d, J = 8 Hz, 1H), 7.45 (br s, 1H), 8.40 (d, J = 6 Hz, 2H).

***N′*-(3-Chlorophenylsulfonyl)-*N*-ethyl-5-(furan-2-yl)-4,5-dihydro-1*H*-pyrazole-1-carboxamidine (19).** Following the same procedure as described for **1**, **63gc** (1.30 g crude, max 3.39 mmol) was reacted with ethylamine (2 mL of a 70% solution in water, excess). The mixture was concentrated under reduced pressure, 5% aqueous $NaHCO_3$ was added, and the mixture was extracted twice with DCM. The combined organic layers were dried over Na_2SO_4, filtered, and concentrated under reduced pressure. The crude product was purified by flash chromatography (DCM, DCM/acetone = 99:1) and subsequently by reverse phase preparative HPLC to give 420 mg (17% over three steps) of **19** as an orange amorphous solid. ^{1}H NMR (400 MHz, $CDCl_3$) δ 1.16 (t, J = 7.1 Hz, 3H), 3.00 (ddd, J = 18.6, 6.4, and 1.7 Hz, 1H), 3.22 (ddd, J = 18.6, 12.0, and 1.6 Hz, 1H), 3.49−3.64 (m, 2H), 5.60 (dd, J = 12.0 and 6.4 Hz, 1H), 6.01 (d, J = 3.2 Hz, 1H), 6.17 (dd, J = 3.2 and 1.7 Hz, 1H), 7.08 (br s, 1H), 7.03 (t, J = 1.6 Hz, 1H), 7.21 (d, J = 1.4 Hz, 1H), 7.29 (t, J = 7.9 Hz, 1H), 7.38−7.42 (m, 1H), 7.56−7.60 (m, 1H), 7.69 (t, J = 1.8 Hz, 1H).

***N′*-(3-Chlorophenylsulfonyl)-*N*-ethyl-5-(4-fluorophenyl)-4,5-dihydro-1*H*-pyrazole-1-carboxamidine (20).** Following the same procedure as described for **1**, **63hc** (8.40 g crude, max 11.87 mmol) was reacted with ethylamine (9.56 mL of a 70% solution in water, excess). The mixture was concentrated under reduced pressure, 5% aqueous $NaHCO_3$ was added, and the mixture was extracted twice with EtOAc. The combined organic layers were dried over $MgSO_4$, filtered, and concentrated under reduced pressure. The crude product was purified by flash chromatography (DCM, DCM/MeOH = 95:5) and subsequently by reverse phase preparative HPLC. The obtained material was triturated with Et_2O/PE = 1:2, and the solids were filtered off and dried in vacuo at 40 °C to give 0.93 g (13% over two steps) of **20** as a yellow solid, mp 139−140 °C. ^{1}H NMR (400 MHz, $CDCl_3$) δ 1.22 (t, J = 7.2 Hz, 3H), 2.70 (dd, J = 6.8 and 1.5 Hz, 1H), 3.36 (dd, J = 11.9 and 1.5 Hz, 1H), 3.55−3.74 (m, 2H), 5.42 (dd, J = 11.9 and 6.8 Hz, 1H), 6.85 (t, J = 8.5 Hz, 2H), 6.91−6.99 (m, 2H), 7.00 (t, J = 1.6 Hz, 1H), 7.14 (t, J = 7.7 Hz, 1H), 7.24 (br s, 1H), 7.31−7.36 (m, 1H), 7.36−7.41 (m, 1H).

***N′*-(3-Chlorophenylsulfonyl)-*N*-(2,2,2-trifluoroethyl)-4-ethyl-4,5-dihydro-1*H*-pyrazole-1-carboxamidine (21).** **63ac** (350 mg, 1.01 mmol) was dissolved in 20 mL of MeOH, and 2,2,2-trifluoroethylamine (805 μL, 10.1 mmol) was added. The mixture was stirred overnight at 60 °C in a sealed tube. The mixture was concentrated under reduced pressure and the crude product was purified by flash chromatography (EtOAc) to give 88 mg (22%) of **21** as a colorless oil. ^{1}H NMR (400 MHz, $CDCl_3$) δ 0.97 (t, J = 7.5 Hz, 3H), 1.16 (t, J = 7.1 Hz, 3H), 1.46−1.69 (m, 2H), 3.07−3.19 (m, 1H), 3.43−3.59 (m, 2H), 3.67 (dd, J = 11.4 and 7.5 Hz, 1H), 4.06 (t, J = 11.2 Hz, 1H), 6.97 (br s, 1H), 6.94 (d, J = 1.8 Hz, 1H), 7.52 (d, J = 8.4 Hz, 1H), 7.76 (dd, J = 8.4 and 2.0 Hz, 1H), 8.03 (d, J = 2.0 Hz, 1H).

***N′*-(3-Chlorophenylsulfonyl)-*N*-methoxy-4-ethyl-4,5-dihydro-1*H*-pyrazole-1-carboxamidine (22).** **63ac** (500 mg, 1.45 mmol) was dissolved in 10 mL of MeOH. *O*-Methylhydroxylamine hydrochloride (1.21 g, 14.5 mmol) and triethylamine (2.43 mL, 17.4 mmol) were added, and the mixture was stirred overnight at 50 °C. The mixture was concentrated under reduced pressure and the residue was purified by flash chromatography (EtOAc/PE = 1:9 to 1:1) to give 160 mg (32%) of **22** as a pale yellow oil. ^{1}H NMR (400 MHz, $CDCl_3$) δ 0.98 (t, J = 7.5 Hz, 3H), 1.47−1.70 (m, 2H), 3.08−3.18 (m, 1H), 3.54 (dd, J = 11.5 and 7.2 Hz, 1H), 3.81 (s, 3H), 3.94 (t, J = 11.5 Hz, 1H), 7.00 (d, J = 1.4 Hz, 1H), 7.40 (t, J = 7.8 Hz, 1H), 7.44−7.48 (m, 1 H), 7.82−7.86 (m, 1H), 7.95 (t, J = 1.8 Hz, 1H), 9.16 (br s, 1H).

***N′*-(4-Chlorophenylsulfonyl)-*N*,4-diethyl-4,5-dihydro-1*H*-pyrazole-1-carboxamidine (23).** Following the same procedure as described for **1**, reaction of **63ad** (750 mg, 2.17 mmol) with ethylamine (3 mL of a 70% solution in water, excess) gave 690 mg (93%) of **23** as pale yellow crystals, mp 84−86 °C. ^{1}H NMR (400 MHz, $CDCl_3$) δ 0.97 (t, J = 7.5 Hz, 3H), 1.15 (t, J = 7.1 Hz, 3H), 1.46−1.69 (m, 2H), 3.12 (dd, J = 10.9 and 7.1 Hz, 1H), 3.43−3.50 (m, 2H), 3.70 (dd, J = 11.4 and 7.5 Hz, 1H), 4.10 (t, J = 11.3 Hz, 1H), 6.81 (br s, 1H), 6.93 (d, J = 1.8 Hz, 1H), 7.42 (m, 2H), 7.88 (m, 2H).

***N′*-(3-Fluorophenylsulfonyl)-*N*,4-diethyl-4,5-dihydro-1*H*-pyrazole-1-carboxamidine (24).** Following the same procedure as described for **1**, reaction of **63ae** (580 mg, 1.52 mmol) with ethylamine (3 mL of a 70% solution in water, excess) gave 570 mg (99%) of **24** as a yellow oil. ^{1}H NMR (400 MHz, $CDCl_3$) δ 0.96 (t, J = 7.7 Hz, 3H), 1.14 (t, J = 7.1 Hz, 3H), 1.45−1.68 (m, 2H), 3.04−3.18 (m, 1H), 3.41−3.51 (m, 2H), 3.70 (dd, J = 11.0 and 7.5 Hz, 1H), 4.10 (t, J = 11.3 Hz, 1H), 6.80 (br s, 1H), 6.92 (d, J = 1.6 Hz, 1H), 7.16 (tdd, J = 8.4, 2.5, and 0.9 Hz, 1H), 7.42 (dt, J = 8.1 and 5.4 Hz, 1H), 7.63 (ddd, J = 8.6, 2.4, and 1.5 Hz, 1H), 7.72 (ddd, J = 7.7, 2.4, and 0.9 Hz, 1H).

***N′*-(3-(Trifluoromethyl)phenylsulfonyl)-*N*,4-diethyl-4,5-dihydro-1*H*-pyrazole-1-carboxamidine (25).** Following the same procedure as described for **1**, reaction of **63af** (500 mg, 1.32 mmol) with ethylamine (1 mL of a 70% solution in water, excess) gave 470 mg (95%) of **25** as a yellow oil. ^{1}H NMR (400 MHz, $CDCl_3$) δ 0.96 (t, J = 7.7 Hz, 3H), 1.14 (t, J = 7.7 Hz, 3H), 1.45−1.68 (m, 2H), 3.07−3.18 (m, 1H), 3.40−3.51 (m, 2H), 3.71 (dd, J = 11.4 and 7.4 Hz, 1H), 4.10 (t, J = 11.4 Hz, 1H), 6.77 (br s, 1H), 6.93 (d, J = 1.6 Hz, 1H), 7.58 (t, J = 7.9 Hz, 1H), 7.72 (d, J = 8.0 Hz, 1H), 8.12 (d, J = 7.9 Hz, 1H), 8.22 (s, 1H).

General Procedure for Parallel Synthesis of *N′*-(Arylsulfonyl)-*N*,4-diethyl-4,5-dihydro-1*H*-pyrazole-1-carboxamidines for Compounds 26, 27, 29−32, 37, and 39. **67a** (205 mg, 1.0 mmol) was taken up in DCM (5.0 mL), and *N*,*N*-diisopropylethylamine (DiPEA) (0.366 mL, 2.1 mmol) was added. To this suspension, a stock solution of the arylsulfonyl chloride (0.9 mmol in 5.0 mL of DCM) was added, and the mixture was agitated overnight at 30 °C. The mixture was extracted against a 2 M aqueous NaOH solution (10 mL), and the organic phase was separated and evaporated to dryness. The residue was taken up in 10 mL of MeOH and sampled onto a preconditioned SCX column (5 g of IST Isolute SCX-3 material of ~0.6 mequiv/g capacity, prepacked in a 25 mL cartridge). The column was eluted with 15 mL of MeOH, and the combined fractions collected during sampling and elution were evaporated to dryness.

***N′*-(*m*-Tolylsulfonyl)-*N*,4-diethyl-4,5-dihydro-1*H*-pyrazole-1-carboxamidine (26).** By use of 3-methylbenzenesulfonyl chloride as reagent in the general procedure described above, 214 mg (66%) of **26** was

isolated. ^{1}H NMR (400 MHz, DMSO-d_6) δ 0.87 (t, J = 7.5 Hz, 3H), 0.96 (t, J = 7.2 Hz, 3H), 1.37−1.60 (m, 2H), 2.37 (s, 3H), 3.16−3.30 (m, 3H), 3.55 (dd, J = 11.1 and 7.0 Hz, 1H), 3.96 (t, J = 10.9 Hz, 1H), 7.30−7.35 (m, 2H), 7.38 (t, J = 7.6 Hz, 1H), 7.59 (d, J = 7.6 Hz, 1H), 7.61 (s, 1H), 7.67 (br s, 1H).

N'-(3-Methoxyphenylsulfonyl)-*N*,4-diethyl-4,5-dihydro-1*H*-pyrazole-1-carboxamidine (27). By use of 3-methoxybenzenesulfonyl chloride as reagent in the general procedure described above, 224 mg (66%) of **27** was isolated. ^{1}H NMR (400 MHz, $CDCl_3$) δ 0.97 (t, J = 7.5 Hz, 3H), 1.15 (t, J = 7.1 Hz, 3H), 1.43−1.73 (m, 2H), 3.04−3.16 (m, 1H), 3.42−3.52 (m, 2H), 3.71 (dd, J = 11.4 and 7.5 Hz, 1H), 3.85 (s, 3H), 4.11 (t, J = 11.4 Hz, 1H), 6.85 (br s, 1H), 6.92 (d, J = 1.5 Hz, 1H), 6.99−7.03 (m, 1H), 7.35 (t, J = 7.9 Hz, 1H), 7.47−7.49 (m, 1H), 7.51−7.55 (m, 1H).

N'-(3,4-Dichlorophenylsulfonyl)-*N*,4-diethyl-4,5-dihydro-1*H*-pyrazole-1-carboxamidine (28). Following the same procedure as described for **1**, reaction of **63ag** (500 mg, 1.31 mmol) with ethylamine (1 mL of a 70% solution in water, excess) gave 500 mg (100%) of **28** as a yellow oil. ^{1}H NMR (400 MHz, $CDCl_3$) δ 0.97 (t, J = 7.5 Hz, 3H), 1.16 (t, J = 7.1 Hz, 3H), 1.46−1.69 (m, 2H), 3.07−3.19 (m, 1H), 3.43−3.59 (m, 2H), 3.67 (dd, J = 11.4 and 7.5 Hz, 1H), 4.06 (t, J = 11.2 Hz, 1H), 6.97 (br s, 1H), 6.94 (d, J = 1.8 Hz, 1H), 7.52 (d, J = 8.4 Hz, 1H), 7.76 (dd, J = 8.4 and 2.0 Hz, 1H), 8.03 (d, J = 2.0 Hz, 1H).

N'-(3,5-Dichlorophenylsulfonyl)-*N*,4-diethyl-4,5-dihydro-1*H*-pyrazole-1-carboxamidine (29). By use of 3,5-dichlorobenzenesulfonyl chloride as reagent in the general procedure described above, 239 mg (63%) of **29** was isolated. ^{1}H NMR (400 MHz, DMSO-d_6) δ 0.87 (t, J = 7.5 Hz, 3H), 0.97 (t, J = 7.2 Hz, 3H), 1.38−1.62 (m, 2H), 3.16−3.30 (m, 3H), 3.54 (dd, J = 11.1 and 7.0 Hz, 1H), 3.96 (t, J = 10.9 Hz, 1H), 7.37 (s, 1H), 7.74 (d, J = 1.6 Hz, 2H), 7.82 (t, J = 1.6 Hz, 1H), 7.96 (br s, 1H).

N'-(2,5-Dichlorophenylsulfonyl)-*N*,4-diethyl-4,5-dihydro-1*H*-pyrazole-1-carboxamidine (30). By use of 2,5-dichlorobenzenesulfonyl chloride as reagent in the general procedure described above, 191 mg (51%) of **30** was isolated. ^{1}H NMR (400 MHz, DMSO-d_6) δ 0.87 (t, J = 7.5 Hz, 3H), 0.95 (t, J = 7.2 Hz, 3H), 1.38−1.61 (m, 2H), 3.17−3.30 (m, 3H), 3.52−3.60 (m, 1H), 3.98 (t, J = 10.9 Hz, 1H), 7.37 (s, 1H), 7.59−7.66 (m, 2H), 7.89 (br s, 1H), 7.95 (d, J = 1.9 Hz, 1H).

N'-(2,6-Dichlorophenylsulfonyl)-*N*,4-diethyl-4,5-dihydro-1*H*-pyrazole-1-carboxamidine (31). By use of 2,6-dichlorobenzenesulfonyl chloride as reagent in the general procedure described above, 155 mg (41%) of **31** was isolated. ^{1}H NMR (400 MHz, $CDCl_3$) δ 0.97 (t, J = 7.4 Hz, 6H), 1.16 (t, J = 7.1 Hz, 3H), 1.46−1.68 (m, 2H), 3.05−3.16 (m, 1H), 3.49 (q, J = 7.2 Hz, 2H), 3.73 (dd, J = 11.6 and 7.4 Hz, 1H), 4.15 (t, J = 11.3 Hz, 1H), 6.83 (br s, 1H), 6.92 (d, J = 1.5 Hz, 1H), 7.21 (dd, J = 7.6 and 8.4 Hz, 1H), 7.40 (d, J = 8.0 Hz, 2H).

N'-(3-Chloro-2-fluorophenylsulfonyl)-*N*,4-diethyl-4,5-dihydro-1*H*-pyrazole-1-carboxamidine (32). By use of 3-chloro-2-fluorobenzenesulfonyl chloride as reagent in the general procedure described above, 199 mg (55%) of **32** was isolated. ^{1}H NMR (400 MHz, DMSO-d_6) δ 0.87 (t, J = 7.5 Hz, 3H), 0.95 (t, J = 7.2 Hz, 3H), 1.38−1.62 (m, 2H), 3.15−3.30 (m, 3H), 3.55 (dd, J = 11.1 and 7.0 Hz, 1H), 3.98 (t, J = 10.9 Hz, 1H), 7.33 (t, J = 7.6 Hz, 1H), 7.38 (s, 1H), 7.77 (t, J = 7.2 Hz, 1H), 7.95 (br t, J = 5.4 Hz, 1H).

N'-(Naphthalen-1-ylsulfonyl)-*N*,4-diethyl-4,5-dihydro-1*H*-pyrazole-1-carboxamidine (33). Following the same procedure as described for **1**, reaction of **63ah** (440 mg, 1.22 mmol) with ethylamine (1 mL of a 70% solution in water, excess) and purification by flash chromatography (DCM/acetone = 98:2) followed by crystallization from cyclohexane/DCM gave 360 mg (83%) of **33** as white crystals, mp 79.0−80.0 °C. ^{1}H NMR (400 MHz, $CDCl_3$) δ 0.90 (t, J = 7.7 Hz, 3H), 1.05 (t, J = 7.7 Hz, 3H), 1.38−1.61 (m, 2H), 2.95−3.06 (m, 1H), 3.33−3.43 (m, 2H), 3.64 (dd, J = 11.4 and 7.4 Hz, 1H), 3.99 (t, J = 11.4 Hz, 1H), 6.88 (br s, 1H), 6.87 (d, J = 1.6 Hz, 1H), 7.49 (dd, J = 8.1 and 7.4 Hz, 1H), 7.54 (ddd, J = 8.1, 6.8, and 1.3 Hz, 1H), 7.61 (ddd, J = 8.4, 6.8, and 1.4 Hz, 1H), 7.89 (d, J = 8.1 Hz, 1H), 7.97 (d, J = 8.2 Hz, 1H), 8.27 (dd, J = 7.3 and 1.3 Hz, 1H), 8.88 (d, J = 8.5 Hz, 1H).

N'-(Naphthalen-2-ylsulfonyl)-*N*,4-diethyl-4,5-dihydro-1*H*-pyrazole-1-carboxamidine (34). Following the same procedure as described for **1**, reaction of **63ai** (400 mg, 1.11 mmol) with ethylamine (1 mL of a 70% solution in water, excess) gave 397 mg (100%) of **34** as a yellow oil. ^{1}H NMR (400 MHz, $CDCl_3$) δ 0.95 (t, J = 7.7 Hz, 3H), 1.14 (t, J = 7.7 Hz, 3H), 1.43−1.62 (m, 2H), 3.02−3.13 (m, 1H), 3.40−3.55 (m, 2H), 3.71 (dd, J = 11.2 and 7.3 Hz, 1H), 4.10 (t, J = 11.2 Hz, 1H), 6.90 (br s, 1H), 6.90 (d, J = 1.6 Hz, 1H), 7.53−7.60 (m, 2H), 7.84−7.98 (m, 4H), 8.47 (d, J = 1.4 Hz, 1H).

N'-(5-Chloro-3-methylbenzo[*b*]thiophen-2-ylsulfonyl)-*N*,4-diethyl-4,5-dihydro-1*H*-pyrazole-1-carboxamidine (35). Following the same procedure as described for **1**, reaction of **63aj** (500 mg, 1.20 mmol) with ethylamine (1 mL of a 70% solution in water, excess) gave 410 mg (83%) of **35** as an off-white foam. ^{1}H NMR (400 MHz, $CDCl_3$) δ 0.98 (t, J = 7.4 Hz, 3H), 1.14 (t, J = 7.7 Hz, 3H), 1.48−1.70 (m, 2H), 2.69 (s, 3H), 3.08−3.19 (m, 1H), 3.47−3.59 (m, 2H), 3.78 (dd, J = 11.2 and 7.6 Hz, 1H), 4.10 (t, J = 11.2 Hz, 1H), 6.84 (br s, 1H), 6.94 (d, J = 1.6 Hz, 1H), 7.37 (dd, J = 8.6 and 2.0 Hz, 1H), 7.71 (d, J = 8.6 Hz, 1H), 7.73 (d, J = 2.0 Hz, 1H).

N'-(6-Chloroimidazo[2,1-*b*]thiazol-5-ylsulfonyl)-*N*,4-diethyl-4,5-dihydro-1*H*-pyrazole-1-carboxamidine (36). Following the same procedure as described for **1**, reaction of **63ak** (380 mg, 0.97 mmol) with ethylamine (1 mL of a 70% solution in water, excess) gave 390 mg (100%) of **36** as a yellow oil. ^{1}H NMR (400 MHz, $CDCl_3$) δ 0.96 (t, J = 7.5 Hz, 3H), 1.17 (t, J = 7.1 Hz, 3H), 1.46−1.69 (m, 2H), 3.04−3.16 (m, 1H), 3.48−3.57 (m, 2H), 3.70 (dd, J = 11.4 and 7.5 Hz, 1H), 4.10 (t, J = 11.3 Hz, 1H), 6.77 (br s, 1H), 6.96 (d, J = 1.5 Hz, 1H), 7.52 (d, J = 4.6 Hz, 1H), 7.98 (d, J = 4.6 Hz, 1H).

N'-(5-Chlorothiophen-2-ylsulfonyl)-*N*,4-diethyl-4,5-dihydro-1*H*-pyrazole-1-carboxamidine (37). By the use of 5-chlorothiophene-2-sulfonyl chloride as reagent in the general procedure described above and subsequent reverse phase preparative HPLC purification, 82 mg (24%) of **37** was isolated. ^{1}H NMR (400 MHz, $CDCl_3$) δ 0.99 (t, J = 7.5 Hz, 3H), 1.20 (t, J = 7.1 Hz, 3H), 1.48−1.71 (m, 2H), 3.08−3.21 (m, 1H), 3.46−3.60 (m, 2H), 3.74 (dd, J = 11.0 and 7.4 Hz, 1H), 4.14 (t, J = 11.0 Hz, 1H), 6.77 (br s, 1H), 6.83 (d, J = 3.9 Hz, 1H), 6.95 (d, J = 1.4 Hz, 1H), 7.35 (d, J = 3.9 Hz, 1H).

N'-(5-Chloro-1,3-dimethyl-1*H*-pyrazol-4-ylsulfonyl)-*N*,4-diethyl-4,5-dihydro-1*H*-pyrazole-1-carboxamidine (38). **67a** (300 mg, 1.47 mmol) was suspended in 10 mL of DCM. Diisopropylethylamine (0.53 mL, 3.08 mmol) and 5-chloro-1,3-dimethyl-1*H*-pyrazole-4-sulfonyl chloride (275 mg, 1.32 mmol) were added, and the mixture was stirred overnight at room temperature. Because of low conversion, acetonitrile (10 mL) was added, the DCM was allowed to evaporate, and the mixture was refluxed overnight. After concentration under reduced pressure, DCM was added and the organic phase was washed with 5% aqueous $NaHCO_3$ followed by 2 M NaOH. The organic layer was dried over Na_2SO_4, filtered, and concentrated under reduced pressure. The crude product was purified by flash chromatography (DCM/acetone = 98:2 to 95:5) to give 130 mg (27%) of **38** as an orange oil. ^{1}H NMR (400 MHz, $CDCl_3$) δ 0.98 (t, J = 7.5 Hz, 3H), 1.17 (t, J = 7.2 Hz, 3H), 1.45−1.71 (m, 2H), 2.46 (s, 3H), 3.02−3.18 (m, 1H), 3.45−3.57 (m, 2H), 3.65−3.74 (m, 1H), 3.79 (s, 3H), 4.11 (t, 1H), 6.89 (br s, 1H), 6.92 (br s, 1H).

N'-(4-(Methylsulfonyl)phenylsulfonyl)-*N*,4-diethyl-4,5-dihydro-1*H*-pyrazole-1-carboxamidine (39). By use of 4-methanesulfonylbenzenesulfonyl chloride as reagent in the general procedure described above, 229 mg (59%) of **39** was isolated. ^{1}H NMR (400 MHz, DMSO-d_6) δ 0.97 (t, J = 7.6 Hz, 3H), 1.16 (t, J = 7.2 Hz, 3H),

1.38−1.62 (m, 2H), 3.19−3.26 (m, 3H), 3.27 (s, 3H), 3.54−3.60 (m, 1H), 3.98 (t, J = 10.8 Hz, 1H), 7.35 (s, 1H), 7.89 (br s, 1H), 8.02−8.09 (m, 4H).

Compounds 40 and 41 from Chiral Separation of 6. The enantiomers of **6** were separated by chiral preparative HPLC. The chiral preparative HPLC system consisted of a 250 mm × 80 mm axial compression column packed with CHIRALCELOK as stationary phase and heptane/ethanol (80:20) as mobile phase. The flow rate used was 215 mL/min, and detection was done by using UV set at a wavelength of 220 nm. The racemate was injected as a solution of 4.5% m/v in heptane/ethanol (70:30).

The first eluting enantiomer **40** was isolated in 67% yield with an ee of 99.6; $[\alpha]_D$ +98 (c 1, MeOH). ^{1}H NMR (400 MHz, $CDCl_3$) data were identical to the spectrum of the racemate (**6**).

The second eluting enantiomer **41** was isolated in 78% yield with an ee of 99.0; $[\alpha]_D$ −95 (c 1, MeOH). ^{1}H NMR (400 MHz, $CDCl_3$) data were identical to the spectrum of the racemate (**6**).

***N′*-(3-Chlorophenylsulfonyl)-*N*-ethyl-4,4-dimethyl-4,5-dihydro-1*H*-pyrazole-1-carboxamidine (42).** Following the same procedure as described for **1**, reaction of **74a** (300 mg, 0.87 mmol) with ethylamine (1 mL of a 70% solution in water, excess) and purification by flash chromatography (DCM, DCM/acetone = 99:1 to 98:2) gave 290 mg (98%) of **42** as a colorless oil. ^{1}H NMR (400 MHz, $CDCl_3$) δ 1.16 (t, J = 7.3 Hz, 3H), 1.23 (s, 6H), 3.42−3.51 (m, 2H), 3.79 (br s, 2H), 6.76 (s, 1H), 6.78 (br s, 1H), 7.39 (t, J = 7.8 Hz, 1H), 7.44 (ddd, J = 8.0, 2.1, and 1.3 Hz, 1H), 7.82 (ddd, J = 7.7, 1.6, and 1.3 Hz, 1H), 7.93 (t, J = 2.0 Hz, 1H).

***N′*-(3-Chlorophenylsulfonyl)-*N*,4,4-triethyl-4,5-dihydro-1*H*-pyrazole-1-carboxamidine (43).** Following the same procedure as described for **1**, reaction of **74b** (540 mg, 1.44 mmol) with ethylamine (2 mL of a 70% solution in water, excess) and purification by extraction (DCM/5% aqueous $NaHCO_3$) gave 520 mg (97%) of **43** as a pale yellow oil. ^{1}H NMR (400 MHz, $CDCl_3$) δ 0.87 (t, J = 7.5 Hz, 6H), 1.15 (t, J = 7.3 Hz, 3H), 1.49−1.64 (m, 4H), 3.41−3.50 (m, 2H), 3.81 (s, 2H), 6.73 (s, 1H), 6.75 (br s, 1H), 7.39 (t, J = 7.8 Hz, 1H), 7.43−7.47 (m, 1H), 7.80−7.85 (m, 1H), 7.94 (t, J = 1.6 Hz, 1H).

***N*-[Ethylamino-(2,3-diaza-spiro[4.4]non-3-en-2-yl)methylidene]-3-chlorobenzenesulfonamide (44).** Following the same procedure as described for **1**, reaction of **74c** (550 mg, 1.48 mmol) with ethylamine (2 mL of a 70% solution in water, excess) and purification by extraction (DCM/water) gave 540 mg (99%) of **44** as a pale yellow oil. ^{1}H NMR (400 MHz, $CDCl_3$) δ 1.16 (t, J = 7.2 Hz, 3H), 1.63−1.85 (m, 10H), 3.42−3.53 (m, 2H), 3.85 (s, 2H), 6.81 (br s, 1H), 6.83 (s, 1H), 7.39 (t, J = 7.8 Hz, 1H), 7.42−7.47 (m, 1H), 7.80−7.85 (m, 1H), 7.93 (t, J = 1.6 Hz, 1H).

***N*-[Ethylamino-(2,3-diaza-spiro[4.5]dec-3-en-2-yl)-methylidene]-3-chlorobenzenesulfonamide (45).** Following the same procedure as described for **1**, reaction of **74d** (300 mg, 0.78 mmol) with ethylamine (2 mL of a 70% solution in water, excess) and purification by flash chromatography (DCM, DCM/acetone = 99:1 to 98:2) gave 200 mg (67%) of **45** as a colorless oil. ^{1}H NMR (400 MHz, $CDCl_3$) δ 1.16 (t, J = 7.2 Hz, 3H), 1.32−1.70 (m, 12H), 3.44−3.53 (m, 2H), 3.80 (s, 2H), 6.83 (br s, 1H), 6.83 (s, 1H), 7.40 (t, J = 7.8 Hz, 1H), 7.43−7.47 (m, 1H), 7.81−7.85 (m, 1H), 7.94 (t, J = 1.6 Hz, 1H).

***N*-[Ethylamino-(8-oxa-2,3-diaza-spiro[4.5]dec-3-en-2-yl)methylidene]-3-chlorobenzenesulfonamide (46).** Following the same procedure as described for **1**, reaction of **74e** (810 mg, 2.09 mmol) with ethylamine (1.2 mL of a 70% solution in water, excess) and purification by flash chromatography (EtOAc) followed by crystallization from diisopropyl ether gave 240 mg (30%) of **46** as white crystals, mp 108−110 °C. ^{1}H NMR (400 MHz, $CDCl_3$) δ 1.17 (t, J = 7.3 Hz, 3H), 1.52−1.59 (m, 2H), 1.80−1.89 (m, 2H), 3.44−3.53 (m, 2H), 3.53−3.60 (m, 2H), 3.83−3.90 (m, 2H), 6.87 (s, 1H), 6.90 (br s, 1H), 7.41 (t, J = 7.8 Hz, 1H), 7.45−7.48 (m, 1H), 7.81−7.85 (m, 1H), 7.93 (t, J = 1.6 Hz, 1H).

***N*-[Ethylamino-(2,3,8-triaza-spiro[4.5]dec-3-en-2-yl)methylidene]-3-chlorobenzenesulfonamide (47).** Following the same procedure as described for **1**, reaction of **74f** (10.20 g, 19.2 mmol) with ethylamine (15.3 mL of a 70% solution in water, 0.19 mol) and purification by flash chromatography (DCM/MeOH = 99:1 to 98:2) gave 6.92 g (75%) of *N*-[ethylamino-(8-benzyl-2,3,8-triaza-spiro[4.5]dec-3-en-2-yl)-methylidene]-3-chlorobenzenesulfonamide as a yellow amorphous compound. ^{1}H NMR (400 MHz, $CDCl_3$) δ 1.16 (t, J = 7.2 Hz, 3H), 1.58 (br d, J = 13.5 Hz, 2H), 1.81 (ddd, J = 13.5, 10.5, and 3.8 Hz, 2H), 2.19 (t, J = 10.8 Hz, 2H), 2.66−2.76 (m, 2H), 3.43−3.53 (m, 4H), 3.84 (br s, 2H), 6.82 (s, 1H), 6.86 (br s, 1H), 7.24−7.35 (m, 5H), 7.40 (t, J = 7.9 Hz, 1H), 7.44−7.48 (m, 1H), 7.81−7.85 (m, 1H), 7.94 (t, J = 1.8 Hz, 1H).

N-[Ethylamino-(8-benzyl-2,3,8-triaza-spiro[4.5]dec-3-en-2-yl)methylidene]-3-chlorobenzenesulfonamide (6.91 g, 14.4 mmol) was dissolved in 50 mL of 1,2-dichloroethane and cooled in an ice bath. Dropwise, 1-chloroethyl chloroformate (1.73 mL, 15.9 mmol) was added and the mixture was stirred for 1 h, keeping the temperature below 5 °C. The mixture was concentrated under reduced pressure and coevaporated three times with toluene. The residue was taken up in 50 mL of MeOH, and the mixture was stirred at room temperature over the weekend. The mixture was concentrated under reduced pressure. EtOAc and 2 M NaOH were added to the residue for extraction, and the organic layer was separated, dried over Na_2SO_4, filtered, and concentrated under reduced pressure. The crude product was purified by flash chromatography (EtOAc/MeOH/25% NH_4OH = 80:20:2 to 70:30:3 to 50:50:5) to give 4.30 g (77%) of **47** as an off-white amorphous compound. ^{1}H NMR (400 MHz, $CDCl_3$) δ 1.17 (t, J = 7.3 Hz, 3H), 1.51−1.59 (m, 2H), 1.69−1.78 (m, 2H), 2.72−2.80 (m, 2H), 2.95−3.04 (m, 2H), 3.43−3.53 (m, 2H), 3.87 (br s, 2H), 6.85 (s, 1H), 6.87 (br s, 1H), 7.41 (t, J = 7.8 Hz, 1H), 7.44−7.48 (m, 1H), 7.81−7.85 (m, 1H), 7.94 (t, J = 1.6 Hz, 1H).

***N′*-(3-Chlorophenylsulfonyl)-*N*-ethyl-4,4-bis(fluoromethyl)-4,5-dihydro-1*H*-pyrazole-1-carboxamidine (48).** Following the same procedure as described for **1**, reaction of **74g** (0.12 g, 0.31 mmol) with ethylamine (0.25 mL of a 70% solution in water, excess) and purification by flash chromatography (DCM, DCM/MeOH = 99:1) gave 0.11 g (93%) of **48** as a pale yellow oil. ^{1}H NMR (400 MHz, $CDCl_3$) δ 1.20 (t, J = 7.3 Hz, 3H), 3.48−3.56 (m, 2H), 3.94 (br s, 2H), 4.50 (dd, J = 46.6 and 9.5 Hz, 2H), 4.53 (dd, J = 47.0 and 9.5 Hz, 2H), 6.91 (s, 1H), 7.00 (br s, 1H), 7.41 (t, J = 7.7 Hz, 1H), 7.45−7.49 (m, 1H), 7.79−7.83 (m, 1H), 7.92 (t, J = 1.7 Hz, 1H).

***N′*-(Phenylsulfonyl)-*N*-ethyl-4,4-dimethyl-4,5-dihydro-1*H*-pyrazole-1-carboxamidine (49).** **75** (500 mg, 2.44 mmol) was suspended in 10 mL of DCM. DiPEA (0.88 mL, 5.13 mmol) and benzenesulfonyl chloride (0.31 mL, 2.44 mmol) were added, and the mixture was stirred overnight at room temperature. The mixture was extracted with 5% aqueous $NaHCO_3$ and subsequently with 2 M NaOH, and the organic layer was dried over Na_2SO_4, filtered, and concentrated under reduced pressure. The crude product was purified by flash chromatography (DCM/MeOH = 99.5:0.5 to 99:1) to give 520 mg (69%) of **49** as an orange oil. ^{1}H NMR (400 MHz, $CDCl_3$) δ 1.15 (t, J = 7.3 Hz, 3H), 1.22 (s, 6H), 3.42−3.51 (m, 2H), 3.79 (br s, 2H), 6.74 (s, 1H), 6.84 (br s, 1H), 7.42−7.51 (m, 3H), 7.92−7.97 (m, 2H).

3-Pyridin-4-ylpropenal (59f). Triphenylphosphoranylidene acetaldehyde (6.08 g, 20.0 mmol) was suspended in 10 mL of dry *N*,*N*-dimethylformamide (DMF). Pyridine-4-carbaldehyde (1.93 mL, 20.0 mmol) was added, and the mixture was stirred overnight at room temperature. The mixture was taken up in EtOAc and washed four times with 5% aqueous $NaHCO_3$. The organic layer was dried over Na_2SO_4, filtered, and concentrated under reduced pressure. The residue was taken up in PE, and the suspension was filtered. The filtrate was concentrated under

reduced pressure to give 1.17 g of **59f** as a crude yellow oil. This material was used in subsequent steps without further purification. ^{1}H NMR (400 MHz, $CDCl_3$) δ 6.85 (dd, J = 16 and 8 Hz, 1H), 7.39−7.46 (m, 3H), 8.72 (d, J = 6 Hz, 2H), 9.78 (d, J = 8 Hz, 1H).

4-Ethyl-4,5-dihydro-1*H*-pyrazole (60a). Hydrazine hydrate (58.0 mL, 1.19 mol) was dissolved in MeOH (300 mL) and cooled in an ice bath. To this mixture, a solution of 2-ethylacrolein (100 g, 1.19 mol) in MeOH (100 mL) was added at such a rate that the temperature was kept below 10 °C. The ice bath was removed and the mixture was stirred overnight at room temperature, after which the MeOH was evaporated under reduced pressure. The product was obtained by vacuum distillation (70−80 °C, 20 mbar) to give 54.9 g (47%) of **60a** as a colorless liquid. ^{1}H NMR (400 MHz, $CDCl_3$) δ 0.98 (t, J = 7 Hz, 3H), 1.43−1.68 (m, 2H), 2.90−3.01 (m, 2H), 3.42−3.53 (m, 1H), 5.38 (br s, 1H), 6.77 (s, 1H).

4-Methyl-4,5-dihydro-1*H*-pyrazole (60b). Following the same procedure as described for **60a**, using CH_3CN as solvent, reaction of hydrazine hydrate (16.65 mL, 0.34 mol) with 2-methylacrolein (24.02 g, 0.34 mol) and purification by vacuum distillation (102−108 °C, 250 mbar) gave 7.0 g (24%) of **60b** as a colorless liquid. ^{1}H NMR (400 MHz, $CDCl_3$) δ 1.18 (d, J = 7 Hz, 3H), 2.90 (t, J = 9 Hz, 1H), 3.00−3.12 (m, 1H), 3.51 (t, J = 9 Hz, 1H), 5.48 (br s, 1H), 6.73 (br s, 1H).

3-Methyl-4,5-dihydro-1*H*-pyrazole (60d). Hydrazine hydrate (29.2 mL, 0.60 mol) was dissolved in MeOH (50 mL). To this solution, methyl vinyl ketone (50 mL, 0.60 mol) was added at such a rate that the temperature was kept below 50 °C. The mixture was stirred for 1 h at 50 °C, after which the MeOH was evaporated under reduced pressure. The product was obtained by vacuum distillation (68−82 °C, 20 mbar) to give 11.8 g (23%) of **60d** as a colorless liquid. ^{1}H NMR (400 MHz, DMSO-d_6) δ 1.88 (s, 3H), 2.47 (t, J = 10 Hz, 2H), 3.15 (t, J = 10 Hz, 2H), 6.10 (br s, 1H).

5-Phenyl-4,5-dihydro-1*H*-pyrazole (60e). Hydrazine hydrate (9.2 mL, 0.19 mol) was heated to reflux. A solution of cinnamaldehyde (10.0 g, 75.8 mmol) in *t*-BuOH (20 mL) was added dropwise, and the mixture was refluxed overnight. After concentration under reduced pressure, water was added to the residue and the mixture was extracted twice with DCM. The combined organic layers were washed with water, dried over Na_2SO_4, and concentrated under reduced pressure to give 10.46 g (81%) of a yellow oil containing 85% of the desired product **60e**, which was used in subsequent steps without further purification. ^{1}H NMR (200 MHz, $CDCl_3$) δ 2.61−2.80 (m, 1H), 3.03−3.23 (m, 1H), 4.72 (dd, J = 10 and 8 Hz, 1H), 5.83 (br s, 1H), 6.83 (t, J = 1 Hz, 1H), 7.20−7.47 (m, 5H).

4-(4,5-Dihydro-1*H*-pyrazol-5-yl)pyridine (60f). Hydrazine hydrate (4.27 mL, 87.9 mmol) was added to 20 mL of Et_2O. The emulsion was cooled in an ice/salt bath to −10 °C. A solution of **59f** (1.17 g crude, max 8.8 mmol) in 20 mL of Et_2O was added dropwise. The mixture was stirred overnight, slowly reaching room temperature in the melting ice bath. Subsequently, 5% aqueous $NaHCO_3$ was added and the mixture was extracted five times with EtOAc. The combined organic layers were dried over Na_2SO_4, filtered, and concentrated under reduced pressure. The residue was dissolved in MeOH and brought onto a conditioned SCX ion exchange column. The column was washed with MeOH, and the product was eluted with 1 M NH_3 in MeOH. Evaporation yielded 1.23 g (33% over two steps) of **60f** as a brown oil. ^{1}H NMR (400 MHz, $CDCl_3$) δ 2.61−2.71 (m, 1H), 3.15−3.25 (m, 1H), 4.68−4.76 (m, 1H), 6.82 (br s, 1H), 6.83 (br b, 1H), 7.27(d, J = 6 Hz, 2H), 8.57 (d, J = 6 Hz, 2H).

5-(Furan-2-yl)-4,5-dihydro-1*H*-pyrazole (60g). 3-(2-Furyl) acrolein (5.0 g, 40.9 mmol) was dissolved in 25 mL *tert*-butanol. Hydrazine hydrate (4.0 mL, 81.9 mmol) was added, and the reaction mixture was refluxed for 24 h. The mixture was concentrated under reduced pressure. The residue was taken up in DCM and washed twice with 5% aqueous $NaHCO_3$. The organic phase was dried over Na_2SO_4, filtered, and concentrated under reduced pressure to give 5.6 g of a yellow oil containing 45% of the anticipated title compound and 55% of the noncyclized hydrazone intermediate. Additional refluxing for 24 h in *n*-butanol gave, after similar workup, 5.3 g of **60g** as a crude brown oil. This material was used in subsequent steps without further purification. ^{1}H NMR (400 MHz, $CDCl_3$) δ 2.92 (ddd, J = 17, 8, and 2 Hz, 1H), 3.02 (ddd, J = 17, 10, and 2 Hz, 1H), 4.76 (dd, J = 10 and 8 Hz, 1H), 5.78 (br s, 1H), 6.20 (d, J = 3 Hz, 1H), 6.32 (dd, J = 3 and 2 Hz, 1H), 6.87 (br s, 1H), 7.36 (m, 1H).

5-(4-Fluorophenyl)-4,5-dihydro-1*H*-pyrazole (60h). Hydrazine hydrate (13.23 mL, 199.8 mmol) was added to 50 mL of THF. The mixture was cooled to −10 °C. A solution of 4-fluorocinnamaldehyde (3.00 g, 19.98 mmol) in 50 mL of Et_2O was added dropwise. The mixture was stirred overnight, slowly reaching room temperature. Water was added, and the mixture was extracted twice with EtOAc. The combined organic layers were dried over $MgSO_4$, filtered, and concentrated under reduced pressure. The residue was dissolved in MeOH and brought onto a conditioned SCX ion exchange column. The column was washed with MeOH, and the product was eluted with 1 M NH_3 in MeOH. Evaporation yielded 2.15 g (52%) of **60h** as a yellow oil. ^{1}H NMR (400 MHz, $CDCl_3$) δ 2.66 (ddd, J = 17.1, 9.0, and 1.6 Hz, 1H), 3.13 (ddd, J = 17.1, 10.7, and 1.6 Hz, 1H), 4.71 (dd, J = 10.7 and 9.0 Hz, 1H), 5.81 (br s, 1H), 7.02 (t, J = 8.7 Hz, 2H), 7.30 (dd, J = 8.7 and 5.5 Hz, 2H).

***N*-(Bis-methylsulfanylmethylidene)-2-chlorobenzenesulfonamide (62a).** 2-Chlorobenzenesulfonamide (41.6 g, 0.22 mol) and carbon disulfide (22 mL, 0.36 mol) were dissolved in DMF (300 mL), and the mixture was cooled in an ice bath. A solution of KOH (29.0 g 0.52 mol) in water (100 mL) was added dropwise at such a rate that the temperature was kept below 10 °C. The mixture was stirred for 30 min at 5−10 °C. Subsequently, methyl iodide (32 mL, 0.51 mol) was added dropwise at such a rate that the temperature was kept below 10 °C. Then the mixture was allowed to warm to room temperature and stirred for another 30 min. Water (250 mL) was added, and the formed white precipitate was filtered off and washed with water followed by EtOH. Drying in vacuo yielded 42.6 g (66%) of **62a** as white crystals, mp 129−130 °C. ^{1}H NMR (200 MHz, $CDCl_3$) δ 2.57 (s, 6H), 7.32−7.60 (m, 3H), 8.11−8.27 (br d, J = 7.5 Hz, 1H).

Via a similar procedure, compounds **62b**−**k** were synthesized. Full experimental details are provided in the Supporting Information.

***N*-[(4-Ethyl-4,5-dihydro-1*H*-pyrazol-1-yl)methylsulfanylmethylidene]-2-chlorobenzenesulfonamide (63aa).** **60a** (6.7 g, 68.3 mmol) was dissolved in pyridine (100 mL). **62a** (20.2 g, 68.3 mmol) was added, and the mixture was refluxed overnight. The mixture was concentrated under reduced pressure and the crude product was purified by flash chromatography (DCM, DCM/acetone = 99:1 to 95:5) to give 15.6 g (62%) of **63aa** as a yellow oil. ^{1}H NMR (400 MHz, $CDCl_3$) δ 1.02 (t, J = 7 Hz, 3H), 1.55−1.77 (m, 2H), 2.28 (s, 3H), 3.27−3.39 (m, 1H), 4.13 (dd, J = 12 and 7 Hz, 1H), 4.57 (t, J = 12 Hz, 1H), 7.16 (d, J = 2 Hz, 1H), 7.39 (dt, J = 7 and 2 Hz, 1H), 7.46 (dt, J = 7 and 2 Hz, 1H), 7.52 (dd, J = 7 and 2 Hz, 1H), 8.18 (dd, J = 7 and 2 Hz, 1H).

Via a similar procedure, compounds **63ab**, **63ac**, **63ad**, **63ae**, **63af**, **63ag**, **63ah**, **63ai**, **63aj**, **63ak**, **63bc**, **63cc**, **63dc**, **63ec**, **63fc**, **63gc**, and **63hc** were synthesized. Full experimental details are provided in the Supporting Information.

1-Ethyl-*S*-methylisothiourea Hydroiodide (66a). Ethylthiourea (20.5 g, 0.20 mol) was dissolved in 100 mL of EtOH. The mixture was cooled in an ice bath, and MeI (13.5 mL, 0.22 mol) was added dropwise. The mixture was stirred for 1 h at room temperature and concentrated under reduced pressure to give 48.3 g (100%) of **66a** as a light yellow oil. ^{1}H NMR (400 MHz, DMSO-d_6) δ 1.17 (t, J = 7 Hz, 3H), 2.61 (s, 3H), 3.34 (q, J = 7 Hz, 2H), 9.10 (br s, 3H).

***N*′,4-Diethyl-4,5-dihydro-1*H*-pyrazole-1-carboxamidine Hydrochloride (67a).** **60a** (19.36 g, 0.20 mol) was dissolved in 100 mL of toluene. **66a** (48.5 g, 0.20 mol) and diisopropylethylamine

(33.8 mL, 0.20 mol) were added, and the mixture was refluxed for 48 h. After concentration under reduced pressure, 2 M NaOH was added and the mixture was extracted three times with DCM. The combined organic layers were dried over Na_2SO_4, filtered, and concentrated under reduced pressure to yield 32.7 g of a red oil. The oil was dissolved in EtOH, and 1 M HCl in EtOH (194 mL) was added dropwise. The mixture was stirred at room temperature for 30 min and concentrated under reduced pressure. By crystallization from acetonitrile/MtBE = 1:1, 11.52 g (29%) of **67a** was isolated as a beige solid. ^{1}H NMR (400 MHz, DMSO-d_6) δ 0.96 (t, J = 7 Hz, 3H), 1.16 (t, J = 7 Hz, 3H), 1.46−1.73 (m, 2H), 3.28−3.45 (m, 3H), 3.56 (dd, J = 10 and 6 Hz, 1H), 3.98 (t, J = 10 Hz, 1H), 7.33 (br s, 1H), 7.98 (br s, 2H), 8.07 (t, J = 6 Hz, 1H).

2,2-Diethylmalononitrile (70b). Malononitrile (15.2 g, 0.23 mol) was mixed with tetrabutylammonium bromide (3.0 g, 4 mol %) and ethyl iodide (36.8 mL, 0.46 mol). After being stirred for 30 min at room temperature, the mixture was cooled in an ice bath and potassium *tert*-butoxide (51.6 g, 0.46 mol) was added portionwise. The ice bath was removed, and the mixture was stirred for 30 min at room temperature. Water was added, and the aqueous portion was extracted with DCM. The organic layer was dried over Na_2SO_4, filtered, and concentrated under reduced pressure. Purification by flash chromatography (DCM) gave 20.4 g (73%) of **70b** as an orange oil, which solidified upon standing. ^{1}H NMR (400 MHz, $CDCl_3$) δ 1.29 (t, J = 7 Hz, 6H), 2.00 (q, J = 7 Hz, 4H).

Cyclopentane-1,1-dicarbonitrile (70c). Malononitrile (15.0 g, 0.23 mol) was dissolved in 200 mL of dry DMF, and the mixture was cooled in an ice bath. Subsequently, 1,8-diazabicyclo[5.4.0]undec-7-ene (DBU) (75 mL, 0.50 mol) and 1,5-dibromobutane (29.6 mL, 0.25 mol) were added dropwise. The ice bath was removed, extra dry DMF (100 mL) was added to keep the mixture stirrable, and the mixture was heated to 80 °C for 2 h. After cooling, the mixture was poured into DCM and washed five times with 5% aqueous $NaHCO_3$. The organic layer was dried over Na_2SO_4 and concentrated under reduced pressure. The crude product was purified by flash chromatography (PE/EtOAc = 9:1) to give 23.4 g (86%) of **70c** as a colorless liquid. ^{1}H NMR (400 MHz, $CDCl_3$) δ 1.93−2.04 (m, 4H), 2.36−2.48 (m, 4H).

Cyclohexane-1,1-dicarbonitrile (70d). Following the same procedure as described for **70c**, reaction of malononitrile (15.0 g, 0.23 mol) with 1,5-dibromopentane (34 mL, 0.25 mol) in the presence of DBU (75 mL, 0.50 mol) and purification by flash chromatography (PE/EtOAc = 9:1) gave 25.7 g (84%) of **70d** as white crystals. ^{1}H NMR (400 MHz, $CDCl_3$) δ 1.48−1.61 (m, 2H), 1.70−1.82 (m, 4H), 2.12 (t, J = 6 Hz, 4H).

Tetrahydropyran-4,4-dicarbonitrile (70e). Malononitrile (5.0 g, 75.7 mmol) was dissolved in 5 mL of DMSO. Subsequently, bis(2-bromoethyl) ether (9.49 mL, 75.7 mmol) and tetrabutylammonium bromide (1.22 g, 5 mol %) were added, followed by portionwise addition of potassium *tert*-butoxide (8.49 g, 75.7 mmol). The mixture was stirred for 4 h at room temperature, taken up in DCM, and washed 3 times with 5% aqueous $NaHCO_3$. The organic phase was dried over Na_2SO_4, filtered, and concentrated under reduced pressure. The crude material was purified by flash chromatography (PE/Et_2O = 65:35) to give 2.49 g (24%) of **70e** as an off-white solid. ^{1}H NMR (400 MHz, $CDCl_3$) δ 2.24 (t, J = 5.1 Hz, 4H), 3.87 (t, J = 5.1 Hz, 4H).

1-Benzylpiperidine-4,4-dicarbonitrile (70f). Bis-(2-chloroethyl)amine hydrochloride (150.0 g, 0.84 mol) was suspended in 500 mL of acetonitrile. K_2CO_3 (348.4 g, 2.52 mol) and benzyl bromide (99.8 mL, 0.84 mol) were added, and the mixture was refluxed for 24 h. After cooling to room temperature, the mixture was filtered and the filtrate was concentrated under reduced pressure. Purification by flash chromatography (PE, PE/Et_2O = 95:5 to 90:10) gave 46.0 g (21%) of benzyl-bis-(2-chloroethyl)amine as a colorless oil. ^{1}H NMR (400 MHz, $CDCl_3$) δ 2.93 (t, J = 7.0 Hz, 4H), 3.50 (t, J = 7.0 Hz, 4H), 3.74 (s, 2H), 7.29−7.36 (m, 5H).

Malononitrile (12.96 g, 0.20 mol) was dissolved in 250 mL of DMF. K_2CO_3 (29.82 g, 0.22 mol) was added, and the mixture was stirred at 65 °C for 2 h. A solution of benzyl-bis-(2-chloroethyl)amine (46.0 g, 0.20 mmol) in 50 mL of DMF was added dropwise at 65 °C, and the mixture was stirred at 65 °C for another 3 h. After cooling to room temperature, the mixture was diluted with EtOAc and washed three times with 5% aqueous $NaHCO_3$. The organic phase was dried over Na_2SO_4, filtered, and concentrated under reduced pressure to give 25.7 g (56%) of **70f** as a colorless oil. ^{1}H NMR (400 MHz, $CDCl_3$) δ 2.24 (t, J = 5.2 Hz, 4H), 2.64 (br s, 4H), 3.55 (s, 2H), 7.26−7.36 (m, 5H).

2,2-Diethylpropane-1,3-diamine (71b). A suspension of $LiAlH_4$ (4.66 g, 0.123 mol) in 100 mL of dry Et_2O was cooled in an ice bath, and a solution of **70b** (5.0 g, 40.9 mmol) in 50 mL of dry Et_2O was added dropwise at such a rate that the temperature was kept below 20 °C. The mixture was stirred overnight at room temperature, cooled in an ice bath, and quenched by adding water (5 mL), 2 M aqueous NaOH (10 mL), and again water (5 mL). The suspension was filtered, the filter cake was washed with Et_2O, and the combined filtrates were concentrated under reduced pressure to give 5.0 g (94%) of **71b** as a clear, light-yellow liquid. ^{1}H NMR (400 MHz, $CDCl_3$) δ 0.80 (t, J = 8 Hz, 6H), 1.08 (br s 4H), 1.22 (q, J = 8 Hz, 4H), 2.52 (s, 4H).

Via a similar procedure, compounds **71c**, **71d**, and **71f** were synthesized. Full experimental details are provided in the Supporting Information.

(4-(Aminomethyl)tetrahydropyran-4-yl)methanamine (71e). **70e** (1.52 g, 11.2 mmol) was dissolved in 25 mL of dry THF and cooled to −10 °C. Dropwise, a 1 M solution of BH_3 in THF (55.8 mL, 55.8 mmol) was added. The mixture was warmed to room temperature and subsequently stirred for 6 h at 60 °C. The reaction mixture was cooled in an ice bath, quenched by dropwise addition of 6 M aqueous HCl (24.2 mL, 145 mmol), warmed to room temperature, and stirred for 2 h. The mixture was neutralized with 2 M aqueous NaOH and washed three times with DCM. The aqueous layer was concentrated under reduced pressure, and the residue was taken up in $CHCl_3$. The solids were filtered off and the organic phase was concentrated under reduced pressure to give 1.0 g (62%) of **71e** as a yellow oil. ^{1}H NMR (400 MHz, $CDCl_3$) δ 1.43 (br s, 4H), 1.46 (t, J = 5.6 Hz, 4H), 2.73 (s, 4H), 3.67 (t, J = 5.6 Hz, 4H).

4,4-Dimethyl-4,5-dihydro-3*H*-pyrazole (72a). 2,2-Dimethyl-1,3-propanediamine (20.0 g, 0.196 mol) was dissolved in a mixture of water (80 mL) and MeOH (20 mL) and cooled in an ice bath. Simultaneously, 30% aqueous H_2O_2 (120 mL, 1.17 mol) and 10% aqueous NaClO (350 mL, 0.47 mol) were added dropwise. The mixture was stirred overnight at room temperature and extracted with DCM. The organic layer was dried over Na_2SO_4, filtered, and concentrated under reduced pressure. Vacuum distillation (102−105 °C, 250 mbar) gave 11.4 g (59%) of **72a** as a colorless viscous oil. ^{1}H NMR (200 MHz, $CDCl_3$) δ 1.05 (s, 6H), 4.14 (s, 4H).

Via a similar procedure, compounds **72b**−**g** were synthesized. Full experimental details are provided in the Supporting Information.

***N*-[(4,4-Dimethyl-4,5-dihydro-1*H*-pyrazol-1-yl)methylsulfanylmethylidene]-3-chlorobenzenesulfonamide (74a).** Following the same procedure as described for **63aa**, reaction of **72a** (0.23 g, 2.37 mmol) with **62c** (700 mg, 2.37 mmol) and purification by flash chromatography (DCM, DCM/acetone = 99:1 to 98:2) gave 600 mg (73%) of **74a** as white crystals, mp 118.5−119.7 °C. ^{1}H NMR (400 MHz, $CDCl_3$) δ 1.31 (s, 6H), 2.23 (s, 3H), 4.21 (s, 2H), 6.98 (s, 1H), 7.43 (t, J = 8 Hz, 1H), 7.47−7.52 (m, 1H), 7.86 (dt, J = 8 and 2 Hz, 1H), 7.97 (t, J = 2 Hz, 1H).

Via a similar procedure, compounds **74b**−**g** were synthesized. Full experimental details are provided in the Supporting Information.

***N*′-Ethyl-4,4-dimethyl-4,5-dihydro-1*H*-pyrazole-1-carboxamidine Hydrochloride (75).** **72a** (12.0 g, 122 mmol) was dissolved

in 100 mL of pyridine. A solution of **66a** (30.0 g, 122 mmol) in 50 mL of pyridine was added, and the mixture was refluxed for 20 h. The mixture was cooled to room temperature and concentrated under reduced pressure, and the residue was taken up in 120 mL of DCM. The organic phase was extracted with 2 N NaOH (2 × 120 mL), washed with water (120 mL), dried over Na_2SO_4, and evaporated under reduced pressure to yield 16.3 g (max 97 mmol, 79%) of an orange oil. The oil (10.0 g, max 59 mmol) was taken up in 50 mL of EtOAc and heated to 60 °C. After removal of the heat source, 20 mL of a 5−6 N solution of HCl in isopropanol was dosed over 4 min. After the mixture was cooled to room temperature, 50 mL of EtOAc was added over 4 min, and the mixture was stirred at 20 °C for 90 min. The formed crystals were collected by filtration, washed with 20 mL of EtOAc, and dried in vacuo at mild heating to give 6.52 g (32 mmol, 54%) of **75** as a yellow solid. ^{1}H NMR (400 MHz, DMSO-d_6) δ 1.08 (t, J = 7.3 Hz, 3H), 1.15 (s, 6H), 3.08 (q, J = 7.3 Hz, 2H), 3.37 (s, 2H), 6.65 (s, 1H), 8.25 (s, 2H).

In Vitro Affinity for the Human 5-HT$_6$R. Affinity for human 5-HT$_6$ receptors was measured in a membrane preparation of CHO cells transfected with human 5-HT$_6$ receptors by binding studies using [^{3}H]*N*-methyllysergic acid diethylamide ([^{3}H]LSD) as ligand. The membrane preparation was prepared from cells supplied by Eurosscreen (Brussels, Belgium). CHO/Gα16/mtAEQ/h5HT6-A1 cells were grown in T-flasks in CHO-S-SFM II medium (Gibco BRL), supplemented with 1% dialyzed FCS, 2 mM L-glutamine, Geneticin at 500 μg/mL, and Zeocin at 200 μg/mL. Cells were harvested using 0.25% trypsin (1 mL/T175-flask), centrifuged, and subsequently suspended in CHO-S-SFM II medium and frozen at −80 °C. After thawing, cells were centrifuged at 4 °C for 3 min at 1500*g*. From the pellet, cell membranes were prepared by two cycles of homogenization (Potter-Elvehjem 10 strokes, 600 rpm) and centrifugation (40000*g* for 15 min, 4 °C). The assay was established to achieve steady state conditions and to optimize specific binding. For the 5-HT$_6$R, membranes from 5 × 10^5 cells were incubated with 5.0 nM [^{3}H]LSD and test compound at 37 °C for 30 min. Nonspecific binding was determined using 10^{-5} M serotonin. Assays were terminated by vacuum filtration through glass fiber filters (GF/B) that had been pretreated with 0.5% polyethyleneimine. Total and bound radioactivity was determined by liquid scintillation counting. Greater than 80% specific binding was achieved in each of these assays. Compounds were tested at a 4 log concentration range; all determinations were performed as triplicates. IC$_{50}$ values were determined by nonlinear regression analysis using Hill equation curve fitting. The inhibition constants (K_i) were calculated from the Cheng−Prusoff equation:

$$K_i = \frac{IC_{50}}{1 + \frac{L}{K_d}}$$

wherein L represents the concentration radioligand ([^{3}H]LSD) in the assay and K_d the affinity of the radioligand for the receptor. Results are expressed as mean $K_i \pm$ SD from at least three separate experiments.

In Vitro Functional Activity ((Ant)Agonism) on the Human 5-HT$_6$R. The CHO human 5-HT$_6$R aequorin assay was bought from Euroscreen, Brussels, Belgium (Euroscreen, technical dossier, human recombinant serotonin 5-HT$_6$-A1 receptor, DNA clone, and CHO AequoScreen recombinant cell line, catalog no. ES-316-A, February 2003). Human-5-HT$_6$R-aequorin cells express mitochondrial targeted apo-aequorin. Cells have to be loaded with coelanterazine in order to reconstitute active aequorin. After binding of agonists to the human 5-HT$_6$R, the intracellular calcium concentration increases and binding of calcium to the apo-aequorin/coelenterazine complex leads to an oxidation reaction of coelenterazine, which results in the production of apo-aequorin, coelenteramide, CO_2, and light (λ_{max} = 469 nm). This luminescent response is dependent on the agonist concentration. Luminescence is measured using the MicroBeta Jet (Perkin-Elmer). Compounds were dissolved in dimethylsulfoxide (DMSO) at 10 mM and diluted in assay buffer to tested concentrations, with a maximal content of 0.1% (v/v) DMSO. Compounds were tested at a 5 log concentration range, and three independent experiments were performed in duplicate. Agonistic effects of compounds are expressed as pEC$_{50}$. Antagonistic effects of compounds were determined as inhibition of 10^{-8} M α-methylserotonin induced luminescence, and the pA_2 was calculated according to the Cheng−Prusoff equation.

In Vitro Determination of Metabolic Stability in the Presence of Human/Rat Hepatocytes. Pooled human hepatocytes (five males, five females) and pooled rat hepatocytes (male Sprague−Dawley rats) were purchased from Invitrotech (Germany) and Tebu-bio (France), respectively, and were stored in liquid nitrogen prior to use. To obtain an in vitro estimate of biological half-life ($t_{1/2}$), hepatocytes (50 000 cells per well, in 96-well plates) were incubated with test compound (1 μg/mL) in Williams medium E containing 5 μg/mL insulin at 37 °C in a water bath, under an atmosphere of oxygen containing 4−7% CO_2. Final volume per well was 100 μL, and final DMSO concentration (from stock solution of test compound) was kept at ≤0.1% to avoid toxic effects on hepatocytes. Control incubations were included; for each compound tested an incubation without hepatocytes was performed to check for chemical instability. In each test plate, an incubation was performed without compound to check for interfering background, and midazolam was included as reference compound with known characteristics. All incubations were performed in duplicate for each test compound. Compounds were incubated for 0, 10, 20, 40, and 60 min. Reactions were stopped by the addition of 100 μL of ice-cold acetonitrile at the appropriate time points, and the plates were vortexed and put on ice. Incubation plates were centrifuged at 2500 rpm for 5 min at 4 °C to precipitate the protein. The supernatant from each well was pipetted into a collection plate, covered with a rubber cover, and stored at −80 °C until HPLC−MS analysis. After thawing, the samples were mixed and centrifuged at 3500 rpm for 10 min at 4 °C. To measure possible reduction of the concentration of test compounds, samples were injected into a single quadrupole HPLC−MS system (Agilent series 1100 LC-MSD), using a gradient in order to achieve chromatographic separation. In the mass spectrometer, ionization was achieved by ESI, followed by analysis of the formed ions by SIM. Eluent A consisted of 0.77 g of ammonium acetate + 800 mL of water + 100 mL of methanol + 100 mL of acetonitrile. Eluent B consisted of 0.77 g of ammonium acetate + 100 mL of water + 100 mL of methanol + 800 mL of acetonitrile. Table 7 shows the pump gradient and other parameters. The "areas under the curve" at the different incubation times were integrated and plotted against (incubation) time, from which the $t_{1/2}$ was derived. The intrinsic clearance Cl_{int} [(μL/min)/10^6 cells] was calculated as follows: [ln(2)/($t_{1/2}$ in min)](well volume in μL)/(number of cells per well × 10^{-6}) = [0.693/($t_{1/2}$ in min)][100/0.05].

P-Glycoprotein Assay. The capability of the human MDR1 P-glycoprotein pump to translocate compounds over a cellular monolayer of PK1 LLC MDR cells was assessed. The transport method essentially described in the literature[80] was used. Compounds were added at the start of the experiment at 1 μg/mL to one side of the cellular layer. The bottom-to-top transport was measured as well as the top-to-bottom transport. Compound detection was performed using a LC/MS method. The P-glycoprotein (P-gp) factor was expressed as the ratio of the bottom-to-top transport over the top-to-bottom transport; compounds with a P-gp factor of ≥2 are considered to be P-gp substrates. The membrane passage (MP) was expressed as the mean percentage of compound transported from bottom-to-top and from top-to-bottom at 3 h after adding the compound; compounds with a membrane passage of ≥15% are considered to be well permeable.

Receptor Binding and Enzyme Inhibitory Studies. Selectivity profiling of selected compounds was performed at CEREP (Celle l'Evescault, France).[60] Compounds were tested at 10 μM (in duplicate).

Table 7[a]

time (min)	eluent A (%)	eluent B (%)	flow (mL/min)
0.00	100	0	1
3.60	0	100	1
7.20	0	100	1
8.50	100	0	1
11.00	100	0	1

[a] Column: Inertsil 5 ODS-3 100 mm × 3.0 mm (CP22234) equipped with Chromsep Guard column SS 10 mm × 2 mm (CP28141) thermostated at 25 °C. Well plate temperature: 4 °C. Injection volume: 20 μL. Splitter (post column), 1:4. Total run time: 11.0 min. Detection SIM: $(M + H)^+$, $(M - H)^-$, obtained from full scan recording. ESI (pos/neg) spray: 4.0 kV. Fragmentor: 70. Gain: 2.0. Dwell: 700 ms. Nebulizer pressure: 42 psi. Drying gas temperature: 325 °C. Capillary temperature: 325 °C.

For the assays in which no activity was detected (PS or PI of <40%), the compound was tested at least two times at 10 μM. In assays in which the compound was active, it was tested further at lower concentrations to determine an IC_{50}.

Receptor/Ion Channel/Transporter Binding Studies. Affinity for the investigated target was measured in a membrane preparation of cells or tissue with the specific target by binding studies using [^{3}H]ligand. Compounds were dissolved in dimethylsulfoxide (DMSO) at 10 mM and diluted in assay buffer to tested concentrations. Testing was at a 3 log concentration range around a predetermined IC_{50} for the respective assay: e.g., 10, 1, 0.1, and 0.01 μM for IC_{50} of 0.3 μM and 300, 30, 3, and 0.3 nM for one with IC_{50} of 10 nM. All determinations were performed as duplicates. The highest concentration tested for primes was 10 μM. Results were expressed as percentage of total ligand binding and that of nonspecific binding, per concentration of compound tested (in duplicate). From the concentration displacement curves, IC_{50} values were determined by nonlinear regression analysis using Hill equation curve fitting. For receptor binding assays, the inhibition constants (K_i) were calculated from the Cheng−Prusoff equation $K_i = IC_{50}/(1 + L/K_d)$, where L is the concentration of radioligand in the assay and K_d the affinity of the radioligand for the receptor. Results were expressed as pK_i. Compounds with no significant affinity at 10 μM and higher were concluded to be inactive, denoted by pK_i of <5.0.

Enzyme Inhibition Studies. Inhibitory properties of compounds for the investigated enzyme were measured in an enzyme preparation following incubation of compound with the enzyme preparation and the substrate at a specific time and temperature. The enzyme product was measured by a specified method of detection. The results were expressed as a percentage of control specific activity ((measured specific activity/control specific activity) × 100) and as a percentage inhibition of control specific activity (100 − ((measured specific activity/control specific activity) × 100)) obtained in the presence of test compound). From the concentration curves, IC_{50} values were determined by nonlinear regression analysis using Hill equation curve fitting.

Molecular Modeling. All modeling studies were performed on a Linux workstation equipped with two 64-bit 2.2 MHz dual-core AMD Opteron processors. As the majority of the modeling work presented here was performed well before the release of high-resolution crystal structures of human GPCRs,[81] homology modeling was based on the bovine rhodopsin X-ray structure. The initial homology model of the 5-HT_6R was generously provided by the group of Prof. Leonardo Pardo and differs from the bovine rhodopsin X-ray structure (1U19)[82] by simulated Pro, Ser, and Thr kinks in the α helices.[83] This model was further optimized with the Schrödinger modeling package,[84] version 9.0, using the OPLS2005 force field. To this end, structurally diverse 5-HT_6R antagonists from public and proprietary sources were docked in the binding pocket. This was an ongoing process. As the model was in agreement with reported and observed SAR of reference/proprietary compounds, as well as mutagenesis data from the public domain,[43,50,85,86] it was employed for optimization efforts of the *N*′-(arylsulfonyl)pyrazoline-1-carboxamidines. Representatives of novel structures were manually docked in the 5-HT_6R binding pocket and minimized with restraint backbone. Close analogues were subsequently docked in the rigid pocket with GOLD,[87] version 4, and subjected to further minimization, again using the OPLS2005 force field and restraint backbone.

NMR Studies. The presence of an internal hydrogen bond between the compound's guanidine NH and sulfonamide S═O was experimentally confirmed using the method published by Jansma et al.[63] Measurements were performed on a Bruker DRX600 spectrometer, equipped with a CPTCI triple resonance 5 mm cryoprobe and running the Topspin 1.3 software. In short, to a 10 mM solution of each investigated compound dissolved in 0.6 mL of $CDCl_3$ (0.05% tetramethylsilane (TMS), Cambridge Isotope Laboratories Inc.) progressive aliquots of DMSO-d_6 (Cambridge Isotope Laboratories Inc.) were added at 0, 5, 7, 10, 14, 20, 28, 40, 56, and 80 μL, making the final solution 30% v/v DMSO-d_6. The ^{1}H NMR spectrum was recorded at each step. After correction of the TMS reference to 0 ppm, the chemical shifts of the NH proton(s) and other relevant peaks were recorded as a function of the % DMSO. Dilution effects were assessed to have a negligible effect on the studied chemical shifts. Drying the solution on 4−5 Å molecular sieves before the titrations also had no effect on the chemical shift, indicating that water content of the sample in $CDCl_3$ did not influence the measurements.

Guinea Pig QTc Studies. Guinea pigs were, at least 7 days prior to the study, equipped with a telemetry transmitter. Male Dunkin−Hartley guinea pigs, weighing 350−450 g at arrival, were allowed to acclimatize during, at least, 5 days. On the day of surgery, the animals were anesthetized with O_2/N_2O/isoflurane (0.8 L/min/0.8 L/min/3% as induction and 0.8 L/min/0.8 L/min/1.75% as maintenance). A telemetry transmitter (TA11CTA-F-40) was implanted into the peritoneal cavity under sterile conditions. Two electrodes were subcutaneously tunneled to the breast of the animals and attached to the muscle tissue in a lead II configuration, one near the apex of the heart and a second one in the right armpit. Just before and 24 h after surgery, the animals received a subcutaneous dose (7.5 mg per animal) of Baytrill. On the day of the study, three guinea pigs received a subcutaneous or oral dose of the test compound for determining electrocardiogram (ECG) parameters (QT, QTc, and HR). After the animals were transferred from the holding to the test room, they were individually placed in the test cages and allowed to acclimatize for at least 30 min. The test cages were placed on a Data Science International receiver (RA1010), and data acquisition took place by Spike2, version 6 (Cambridge Electronic Design Ltd., Cambridge, U.K.). The ECG signal was checked for suitability after the acclimatization period. After this acclimatization period, a predrug ECG was recorded for at least 30 min. Following the stabilization period, the animals were dosed with test compound or vehicle. During the dosing procedure, the animals were shortly removed from the cages and no ECG signal was recorded. Once the animals were placed back into the test cages, ECG recording began for 120 min. Subsequently the animals were removed from the test cages and returned to their holding cage.

Per animal, the ECG signal was analyzed for both the stabilization period (30 min) and the compound or vehicle period (120 min). The ECG parameters were evaluated at 300 s intervals. At each time point, five RR intervals and five QT intervals were measured. The following variables from the lead II ECG were determined: RR interval; QT interval; QTc interval ($QTc = QT/(RR)^{1/2}$, Bazett's correction[88]); heart rate (based on RR interval). The following calculations were performed based on the ECG data: (1) Per 300 s interval time point the mean of five consecutive ECG complexes (RR, QT, QTc, and HR) were

calculated. (2) An overall mean predrug value was estimated per ECG parameter. The overall mean predrug value was calculated using mean values calculated per 5 min interval each based on 5 consecutive ECG complexes. (3) Per 300 s interval time point the difference between QTc and mean predrug was calculated (Δ QTc). (4) The effect of the test substance on QTc was expressed as AUC_{120} and E_{max}. The AUC per time point was determined by multiplying the mean of two consecutive Δ QTc values by 5 (=300 s interval expressed as minute). The AUC_{120} was calculated by summing all AUCs. The E_{max} was the highest Δ QTc value after test substance treatment. (5) For each time point, the HR was expressed as percentage relative to the predrug value.

Rat Pharmacokinetics. Preliminary kinetic data in rats were gathered by administration of 1 mg/kg intravenously and 10 mg/kg orally or intraperitoneally to Wistar rats. A group of 10 animals received 1 mg/kg intravenously (2 mL/kg, formulated in 25% 2-hydroxypropyl-β-cyclodextrin (HPCD)). Blood samples were taken at time points 10, 30, 60, 180, and 420 min after dosing, two animals per time point, and at 1440 min after dosing (same two animals sampled at 10 min). After wash-out, the same 10 animals received 10 mg/kg orally (10 mL/kg, formulated in 1% methylcellulose (MC)). Blood and brain samples were taken at 30, 60, 180, 420, and 1440 min after dosing. Another group of 10 animals received 10 mg/kg intraperitoneally (2 mL/kg, formulated in 1% MC + 5% mannitol). Blood and brain samples were taken at 30, 60, 180, 420, and 1440 min after dosing. Plasma samples, after liquid−liquid extraction, were analyzed using a generic bioanalytical method on a TurboFlow MS/MS system. Brain samples were analyzed on the same system after homogenization and solid-phase extraction. Levels in the samples were calculated from a concentration versus response curve obtained from spiked blank matrix samples, which were processed and analyzed in the same way as the samples (extracted calibration curve). The CNS/plasma ratio was estimated using the plasma (ng/mL) over brain (ng/g) concentration over the entire oral dosing time range.

Determination of Fraction Unbound Brain. A literature procedure[89] was followed with modifications. Rat brain was homogenized 1:6 with phosphate-buffered saline (PBS) and spiked with 1 μM test compound; 300 μL of the spiked brain homogenate was dialyzed against 500 μL of PBS in the rapid equilibrium dialysis device for 6 h at room temperature while shaking. After that time point, an aliquot of 60 μL was taken from each well; 60 μL of PBS was added to the wells containing brain homogenate, and 60 μL of brain homogenate was added to the wells containing PBS to adjust the matrices for analysis. Ethanol (240 μL/well) was used for quenching, and samples were frozen until HPLC/MS−MS analysis to measure the AUC of the parent. The fraction of unbound brain was calculated as follows:

$$\%\,\text{free} = (\text{AUC buffer chamber}/\text{AUC brain homogenate chamber}) \times 100$$

$$\%\,\text{bound} = 100 - \%\,\text{free}$$

$$f_{u,\text{homogenate}} = 1 - (\%\,\text{bound}/100)$$

$$\text{undiluted } f_{u,\text{brain}} = (1/D)/[(1/f_{u,\text{homogenate}} - 1) + 1/D]$$

where D is the dilution factor for the brain homogenate.

■ ASSOCIATED CONTENT

Supporting Information. Selectivity profiling of compounds **6**, **14**, **42**, and **47** (Cerep data); synthesis scheme, experimental procedures, and analytical data for intermediate **71g**; detailed experimental information for intermediates not fully described in the Experimental Section. This material is available free of charge via the Internet at http://pubs.acs.org.

■ AUTHOR INFORMATION

Corresponding Author

*Phone: +31-36-5368020. E-mail: arnold.vanloevezijn@online.nl. Address: Salsastraat 179, 1326 LW Almere, The Netherlands.

Present Addresses

†Astra Tech Benelux B.V., Signaalrood 55, 2718 SG Zoetermeer, The Netherlands.

‡Lipid Nutrition B.V., Hogeweg 1, 1521 AZ Wormerveer, The Netherlands.

■ ACKNOWLEDGMENT

The authors thank Christiaan Salomons for LC−MS purity analyses, Jan Hoogendoorn for chiral preparative HPLC separations, Gerard Vollebregt and Martin Haazelager for 5-HT_6R binding and functional assay data, Annemieke Rensink and Pieter Spaans for hepatocyte assay data, Tiny Adolfs and Sander Vader for guinea pig QTc data, Jessica Dijksman for rat PK data, Gisela Backfisch and Renate Anthes (Abbott GmbH & Co. KG, Ludwigshafen, Germany) for fraction unbound brain data, and Huub Nievelstein for valuable pharmacological input.

■ ABBREVIATIONS USED

5-HT_6R, 5-hydroxytryptamine (serotonin) 6 receptor; ACE-Cl, 1-chloroethyl chloroformate; AChEI, acetylcholinesterase inhibitor; AD, Alzheimer's disease; ADME, absorption, distribution, metabolism, and excretion; Bn, benzyl; Boc, *tert*-butoxycarbonyl; CHO, Chinese hamster ovary; CIAS, cognitive impairment associated with schizophrenia; CNS, central nervous system; CYP, cytochrome P450; DBU, 1,8-diazabicyclo[5.4.0]undec-7-ene; DCM, dichloromethane; DiPEA, *N*,*N*-diisopropylethylamine; DMF, *N*,*N*-dimethylformamide; DMSO, dimethylsulfoxide; ECG, electrocardiogram; ELSD, evaporative light scattering detector; GABA, γ-aminobutyric acid; GPCR, G-protein-coupled receptor; hERG, human ether-a-go-go-related gene (Kv11.1 potassium ion channel); HPCD, 2-hydroxypropyl-β-cyclodextrin; HPLC, high performance liquid chromatography; HTS, high throughput screening; id, intraduodenal; ip, intraperitoneal; iv, intravenous; ivp, intravenoportal; LC−MS, liquid chromatography−mass spectrometry; MC, methylcellulose; MtBE, methyl *tert*-butyl ether; NMR, nuclear magnetic resonance; po, per os (oral); PE, petroleum ether (boiling range 40−60 °C); PBS, phosphate buffered saline; P-gp, P-glycoprotein; PK, pharmacokinetics; PSA, polar surface area; QTOF, quadrupole time-of-flight; SAR, structure−activity relationship; SCX, strong cation exchange; THF, tetrahydrofuran; TLC, thin layer chromatography; TMS, tetramethylsilane; UV, ultraviolet

■ REFERENCES

(1) Monsma, F. J., Jr.; Shen, Y.; Ward, R. P.; Hamblin, M. W.; Sibley, D. R. Cloning and expression of a novel serotonin receptor with high affinity for tricyclic psychotropic drugs. *Mol. Pharmacol.* **1993**, *43*, 320–327.

(2) Ruat, M.; Traiffort, E.; Arrang, J. M.; Tardivel-Lacombe, J.; Diaz, J.; Leurs, R.; Schwartz, J. C. A novel rat serotonin (5-HT6) receptor: molecular cloning, localization and stimulation of cAMP accumulation. *Biochem. Biophys. Res. Commun.* **1993**, *193*, 268–276.

(3) Woolley, M. L.; Marsden, C. A.; Fone, K. C. 5-ht6 receptors. *Curr. Drug Targets: CNS Neurol. Disord.* **2004**, *3*, 59–79.

(4) Davies, S.; Silvestre, J. S.; Guitart, X. Drug discovery targets: 5-HT_6 receptor. *Drugs Future* **2005**, *30*, 479.

(5) King, M. V.; Marsden, C. A.; Fone, K. C. A role for the 5-HT_{1A}, 5-HT_4 and 5-HT_6 receptors in learning and memory. *Trends Pharmacol. Sci.* **2008**, *29*, 482–492.
(6) Nichols, D. E.; Nichols, C. D. Serotonin receptors. *Chem. Rev.* **2008**, *108*, 1614–1641.
(7) Borsini, F.; Bordi, F.; Riccioni, T. 5-HT_6 pharmacology inconsistencies. *Pharmacol., Biochem. Behav.* **2011**, *98*, 169–172.
(8) Roth, B. L.; Hanizavareh, S. M.; Blum, A. E. Serotonin receptors represent highly favorable molecular targets for cognitive enhancement in schizophrenia and other disorders. *Psychopharmacology* **2004**, *174*, 17–24.
(9) Mitchell, E. S.; Neumaier, J. F. 5-HT_6 receptors: a novel target for cognitive enhancement. *Pharmacol. Ther.* **2005**, *108*, 320–333.
(10) Upton, N.; Chuang, T. T.; Hunter, A. J.; Virley, D. J. 5-HT_6 receptor antagonists as novel cognitive enhancing agents for Alzheimer's disease. *Neurotherapeutics* **2008**, *5*, 458–469.
(11) Geldenhuys, W. J.; van der Schyf, C. J. Serotonin 5-HT_6 receptor antagonists for the treatment of Alzheimer's disease. *Curr. Top. Med. Chem.* **2008**, *8*, 1035–1048.
(12) Fone, K. C. F. An update on the role of the 5-hydroxytryptamine$_6$ receptor in cognitive function. *Neuropharmacology* **2008**, *55*, 1015–1022.
(13) Johnson, C. N.; Ahmed, M.; Miller, N. D. 5-HT_6 receptor antagonists: prospects for the treatment of cognitive disorders including dementia. *Curr. Opin. Drug Discovery Dev.* **2008**, *11*, 642–654.
(14) Liu, K. G.; Robichaud, A. J. 5-HT_6 antagonists as potential treatment for cognitive dysfunction. *Drug Dev. Res.* **2009**, *70*, 145–168.
(15) Wilson, C.; Terry, A. V., Jr. Enhancing cognition in neurological disorders: potential usefulness of 5-HT_6 antagonists. *Drugs Future* **2009**, *34*, 969–975.
(16) Geldenhuys, W. J.; van der Schyf, C. J. The serotonin 5-HT_6 receptor: a viable drug target for treating cognitive deficits in Alzheimer's disease. *Expert Rev. Neurother.* **2009**, *9*, 1073–1085.
(17) Rossé, G.; Schaffhauser, H. 5-HT_6 receptor antagonists as potential therapeutics for cognitive impairment. *Curr. Top. Med. Chem.* **2010**, *10*, 207–221.
(18) Foley, A. G.; Murphy, K. J.; Hirst, W. D.; Gallagher, H. C.; Hagan, J. J.; Upton, N; Walsh, F. S.; Regan, C. M. The 5-HT_6 antagonists SB-271046 and SB-399885 increase basal and learning induced hippocampal ncam polysialylation. *Int. J. Neuropsychopharmacol.* **2004**, *7*, 215.
(19) Foley, A. G.; Hirst, W. D.; Gallagher, H. C.; Barry, C.; Hagan, J. J.; Upton, N.; Walsh, F. S.; Hunter, A. J.; Regan, C. M. The selective 5-HT_6 receptor antagonists SB-271046 and SB-399885 potentiate NCAM PSA immunolabeling of dentate granule cells, but not neurogenesis, in the hippocampal formation of mature Wistar rats. *Neuropharmacology* **2008**, *54*, 1166–1174.
(20) de Foubert, G.; O'Neill, M. J.; Zetterström, T. S. C. Acute onset by 5-HT_6-receptor activation on rat brain BDNF and Arc mRNA expression. *Neuroscience* **2007**, *147*, 778–785.
(21) Johnson, C. N.; Roland, A.; Upton, N. New symptomatic strategies in Alzheimer's disease. *Drug Discovery Today: Ther. Strategies* **2004**, *1*, 13–19.
(22) Maher-Edwards, G.; Zvartau-Hind, M.; Hunter, A. J.; Gold, M.; Hopton, G.; Jacobs, G.; Davy, M.; Williams, P. Double-blind, controlled phase II study of a 5-HT_6 receptor antagonist, SB-742457, in Alzheimer's disease. *Curr. Alzheimer Res.* **2010**, *7*, 374–385.
(23) Wesołowska, A.; Jastrzębska-Więsek, M. Behavioral pharmacology: potential antidepressant and anxiolytic properties. *Int. Rev. Neurobiol.* **2011**, *96*, 49–71.
(24) Callahan, P. M.; Ilch, C. P.; Rowe, W. B.; Tehim, A. Characterization of the selective 5-HT_6 receptor antagonist SB-271046 in behavioral models of cognition. *Soc. Neurosci. Abstr.* **2004**, 776.19 (abstract).
(25) Comery, T. A.; Schechter, L. E. Method for the Treatment of Cognitive Dysfunction. WO 2007/087151, 2007.
(26) Marcos, B.; Chuang, T. T.; Gil-Bea, F. J.; Ramirez, M. J. Effects of 5-HT_6 receptor antagonism and cholinesterase inhibition in models of cognitive impairment in the rat. *Br. J. Pharmacol.* **2008**, *155*, 434–440.
(27) Mitchell, E. S. 5-HT_6 receptor ligands as antidementia drugs. *Int. Rev. Neurobiol.* **2011**, *96*, 163–187.
(28) Keefe, R. S. E.; Malhotra, A. K.; Meltzer, H. Y.; Kane, J. M.; Buchanan, R. W.; Murthy, A.; Sovel, M.; Li, C.; Goldman, R. Efficacy and safety of donepezil in patients with schizophrenia or schizoaffective disorder: significant placebo/practice effects in a 12-week, randomized, double-blind, placebo-controlled trial. *Neuropsychopharmacology* **2008**, *33*, 1217–1228.
(29) Marder, S. R.; Fenton, W.; Youens, K. Cognition in schizophrenia: the MATRICS initiative. *Am. J. Psychiatry* **2004**, *161*, 25.
(30) Dawson, L. A. The central role of 5-HT_6 receptors in modulating brain neurochemsitry. *Int. Rev. Neurobiol.* **2011**, *96*, 1–26.
(31) Neale, A. C.; Jenkins, H.; Amend, D.; Lesem, M. A 14-day, dose-escalation, double blind, randomized, placebo-controlled study of SGS-518 in adult patients with schizophrenia. *Neuropsychopharmacology* **2005**, *30*, S54.
(32) Arnt, J.; Olsen, C. K. 5-HT_6 receptor ligands and their antipsychotic potential. *Int. Rev. Neurobiol.* **2011**, *96*, 141–161.
(33) Batel, P. Addiction and schizophrenia. *Eur. Psychiatry* **2000**, *15*, 115–122.
(34) Di Chiara, G.; Valentini, V.; Fenu, S. Behavioral and neurochemical pharmacology of 5-HT_6 receptors related to reward and reinforcement. *Int. Rev. Neurobiol.* **2011**, *96*, 111–139.
(35) de Bruin, N. M. W. J.; van Loevezijn, A.; Wijnen, J.; Herremans, A. H. J.; Kruse, C. G. Use of 5-HT6 Antagonists To Prevent Relapse into Addiction. WO 2008/087123, 2008.
(36) van Gaalen, M. M.; Schetters, D.; Schoffelmeer, A. N. M.; de Vries, T. J. 5-HT_6 antagonism attenuates cue-induced relapse to cocaine seeking without affecting cocaine reinforcement. *Int. J. Neuropsychopharmacol.* **2010**, *13*, 961–965.
(37) de Bruin, N. M. W. J.; Kloeze, B. M.; McCreary, A. C. The 5-HT_6 serotonin receptor antagonist SB-271046 attenuates development and expression of nicotine-induced locomotor sensitization in Wistar rats. *Neuropharmacology* **2011**, *61*, 451–457.
(38) Taylor, D.; McAskill, R. Atypical antipsychotics and weight gain: a systematic review. *Acta Psychiatr. Scand.* **2000**, *101*, 416–432.
(39) Heal, D. J.; Smith, S. L.; Fisas, A.; Codony, X.; Buschmann, H. Selective 5-HT_6 receptor ligands: progress in the development of a novel pharmacological approach to the treatment of obesity and related metabolic disorders. *Pharmacol. Ther.* **2008**, *117*, 207–231.
(40) Heal, D.; Gosden, J.; Smith, S. The 5-HT_6 receptor as a target for developing novel antiobesity drugs. *Int. Rev. Neurobiol.* **2011**, *96*, 73–109.
(41) Holenz, J.; Mercè, R.; Díaz, J. L.; Guitart, X.; Codony, X.; Dordal, A.; Romero, G.; Torrens, A.; Mas, J.; Andaluz, B.; Hernández, S.; Monroy, X.; Sánchez, E.; Hernández, E.; Pérez, R.; Cubí, R.; Sanfeliu, O.; Buschmann, H. Medicinal chemistry driven approaches toward novel and selective serotonin 5-HT_6 receptor ligands. *J. Med. Chem.* **2005**, *48*, 1781–1795.
(42) López-Rodríguez, M. L.; Benhamú, B.; de la Fuente, T.; Sanz, A.; Pardo, L.; Campillo, M. A three-dimensional pharmacophore model for 5-hydroxytryptamine$_6$ (5-HT_6) receptor antagonists. *J. Med. Chem.* **2005**, *48*, 4216–4219.
(43) Boess, F. G.; Monsma, F. J., Jr.; Sleight, A. J. Identification of residues in transmembrane regions III and VI that contribute to the ligand binding site of the serotonin 5-HT_6 receptor. *J. Neurochem.* **1998**, *71*, 2169–2177.
(44) Data from Thomson Reuters Integrity, http://www.thomsonreutersintegrity.com/.
(45) Wu, Y.-J.; He, H.; Hu, S.; Huang, Y.; Scola, P. M.; Grant-Young, K.; Bertekap, R. L.; Wu, D.; Gao, Q.; Li, Y.; Klakouski, C.; Westphal, R. S. Identification of a potent and selective 5-HT_6 antagonist: one-step synthesis of (*E*)-3-(benzenesulfonyl)-2-(methylsulfanyl)pyrido[1,2-*a*]pyrimidin-4-ylidenamine from 2-(benzenesulfonyl)-3,3-bis(methylsulfanyl)acrylonitrile. *J. Med. Chem.* **2003**, *46*, 4834–4837.
(46) Kim, H.-J.; Doddareddy, M. R.; Choo, H.; Cho, Y. S.; No, K. T.; Park, W.-K.; Pae, A. N. New serotonin 5-HT_6 ligands from common feature pharmacophore hypotheses. *J. Chem. Inf. Model.* **2008**, *48*, 197–206.
(47) Ivachtchenko, A. V.; Golovina, E. S.; Kadieva, M. G.; Koryakova, A. G.; Kovalenko, S. M.; Mitkin, O. D.; Okun, I. M.; Ravnyeyko, I. M.;

Tkachenko, S. E.; Zaremba, O. V. Synthesis and biological study of 3-(phenylsulfonyl)thieno[2,3-*e*][1,2,3]triazolo[1,5-*a*]pyrimidines as potent and selective serotonin 5-HT_6 receptor antagonists. *Bioorg. Med. Chem.* **2010**, *18*, 5282–5290.

(48) Ivachtchenko, A. V.; Golovina, E. S.; Kadieva, M. G.; Koryakova, A. G.; Kovalenko, S. M.; Mitkin, O. D.; Okun, I. M.; Ravnyeyko, I. M.; Tkachenko, S. E.; Zaremba, O. V. Solution phase parallel synthesis of substituted 3-phenylsulfonyl-[1,2,3]triazolo[1,5-*a*]quinazolines: selective serotonin 5-HT_6 receptor antagonists. *J. Comb. Chem.* **2010**, *12*, 445–452.

(49) Ivachtchenko, A. V.; Dmitriev, D. E.; Golovina, E. S.; Dubrovskaya, E. S.; Kadieva, M. G.; Koryakova, A. G.; Kysil, V. M.; Mitkin, O. D.; Tkachenko, S. E.; Okun, I. M.; Vorobiov, A. A. Synthesis of cycloalkane-annelated 3-phenylsulfonyl-pyrazolo[1,5-*a*]pyrimidines and their evaluation as 5-HT_6 receptor antagonists. *Bioorg. Med. Chem. Lett.* **2010**, *20*, 2133–2136.

(50) Harris, R. N., III; Stabler, R. S.; Repke, D. B.; Kress, J. M.; Walker, K. A.; Martin, R. S.; Brothers, J. M.; Ilnicka, M.; Lee, S. W.; Mirzadegan, T. Highly potent, non-basic 5-HT_6 ligands. Site mutagenesis evidence for a second binding mode at 5-HT_6 for antagonism. *Bioorg. Med. Chem. Lett.* **2010**, *20*, 3436–3440.

(51) Aronov, A. M. Predictive in silico modeling for hERG channel blockers. *Drug Discovery Today: BIOSILICO* **2005**, *10*, 149–155.

(52) Farid, R.; Day, T.; Friesner, R. A.; Pearlstein, R. A. New insights about HERG blockade obtained from protein modeling, potential mapping, and docking studies. *Bioorg. Med. Chem.* **2006**, *14*, 3160–3173.

(53) Imai, Y. N.; Ryu, S.; Oiki, S. Docking model of drug binding to the human ether-a-go-go potassium channel guided by tandem dimmer mutant patch-clamp data: a synergistic approach. *J. Med. Chem.* **2009**, *52*, 1630–1638.

(54) Kongsamut, S.; Kang, J.; Chen, X.-L.; Roehr, J.; Rampe, D. A comparison of the receptor binding and HERG channel affinities for a series of antipsychotic drugs. *Eur. J. Pharmacol.* **2002**, *450*, 37–41.

(55) Silvestre, J. S.; Prous, J. R. Comparative evaluation of potassium hERG channel blockade by antipsychotics. *Methods Find. Exp. Clin. Pharmacol.* **2007**, *29*, 457–465.

(56) Lange, J. H. M.; Coolen, H. K. A. C.; van Stuivenberg, H. H.; Dijksman, J. A. R.; Herremans, A. H. J.; Ronken, E.; Keizer, H. G.; Tipker, K.; McCreary, A. C.; Veerman, W.; Wals, H. C.; Stork, B.; Verveer, P. C.; den Hartog, A. P.; de Jong, N. M. J.; Adolfs, T. J. P.; Hoogendoorn, J.; Kruse, C. G. Synthesis, biological properties, and molecular modeling investigations of novel 3,4-diarylpyrazolines as potent and selective CB_1 cannabinoid receptor antagonists. *J. Med. Chem.* **2004**, *47*, 627–643.

(57) Grosscurt, A. C.; van Hes, R.; Wellinga, K. 1-Phenylcarbamoyl-2-pyrazolines, a new class of insecticides. 3. Synthesis and insecticidal properties of 3,4-diphenyl-1-phenylcarbamoyl-2-pyrazolines. *J. Agric. Food. Chem.* **1979**, *27*, 406–409.

(58) In an effort to measure the basicity and acidity of the sulfonylguaninde core moiety in **6**, no pK_a could be determined experimentally between pH 2 and pH 12, confirming calculations previously carried out with hit structure **1**. Consequently, the pH-metric log *P* of **6** could not be determined. Alternatively, the HPLC log *D* was determined to be 2.4 at Sirius (http://www.sirius-analytical.com), being in reasonable agreement with the AlogP of 2.73 as calculated with Pipeline Pilot (http://accelrys.com).

(59) Currents were measured by using the whole-cell variant of the patch clamp method according to the method described in the following: Crumb, W.; Llorca, P.-M.; Lancon, C.; Thomas, G. P.; Garay, R. P.; Hameg, A. Effects of cyamemazine on hERG, INa, ICa, Ito, Isus and IK1 channel currents, and on the QTc interval in guinea pigs. *Eur. J. Pharmacol.* **2006**, *532*, 270–278.

(60) http://www.cerep.fr/Cerep/Users/index.asp.

(61) Topiol, S.; Sabio, M. X-ray structure breakthroughs in the GPCR transmembrane region. *Biochem. Pharmacol.* **2009**, *78*, 11–20.

(62) For a comprehensive consideration of the effects of intramolecular hydrogen bonding on conformational restrictions in target−ligand interactions and on ligand physicochemical properties see the following: Kuhn, B.; Mohr, P.; Stahl, M. Intramolecular hydrogen bonding in medicinal chemistry. *J. Med. Chem.* **2010**, *53*, 2601–2611.

(63) Jansma, A.; Zhang, Q.; Li, B.; Ding, Q.; Uno, T.; Bursulaya, B.; Liu, Y.; Furet, P.; Gray, N.; Geierstanger, H. Verification of a designed intromolecular hydrogen bond in a drug scaffold by nuclear magnetic resonance. *J. Med. Chem.* **2007**, *50*, 5875–5877.

(64) Flack, H. D. On enantiomorph-polarity estimation. *Acta Crystallogr., Sect. A* **1983**, *39*, 876–881.

(65) Hooft, R. W. W.; Straver, L. H.; Spek, A. L. Determination of absolute structure using Bayesian statistics on Bijvoet differences. *J. Appl. Crystallogr.* **2008**, *41*, 96–103.

(66) *MetaSite*, version 2.7.5; Molecular Discovery Ltd.: Perugia, Italy, 2006. For more background, see the following: Cruciani, G.; Carosati, E.; De Boeck, B.; Ethirajulu, K.; Mackie, C.; Howe, T.; Vianello, R. MetaSite: understanding metabolism in human cytochromes from the perspective of the chemist. *J. Med. Chem.* **2005**, *48*, 6970–6979.

(67) http://www.cyprotex.com/cloescreen/in-vitro-metabolism/cytochrome-p450-reaction-phenotyping/.

(68) Carsky, P.; Hünig, S.; Stemmler, I.; Scheutzow, D. Two step redox systems, XXVII. Vinylogous bipyridyls and biquinolyls; syntheses and UV/VIS-spectra. *Liebigs Ann. Chem.* **1980**, *2*, 291–304.

(69) van de Waterbeemd, H.; Camenisch, G.; Folkers, G.; Chretien, J. R.; Raevsky, O. A. Estimation of blood−brain barrier crossing of drugs using molecular size and shape, and H-bonding descriptors. *J. Drug Targeting* **1998**, *6*, 151–165.

(70) Tsai, T.-Y.; Shia, K.-S.; Liu, H.-J. A facile method for the construction of highly substituted acetonitriles and olefins. Malononitriles as acetonitrile carbanion and alkylidene dianion equivalents. *Synlett* **2003**, 97–101.

(71) Diez-Barra, E.; de la Hoz, A.; Moreno, A.; Sanchez-Verdu, P. Phase transfer catalysis without solvent. Synthesis of cycloalkane-1,1-dicarbonitriles and alkanetetracarbonitriles. *J. Chem. Soc., Perkin Trans. 1* **1991**, *4*, 2593–2596.

(72) Briggs, C. B. A.; Newington, I. M.; Pitt, A. R. Synthesis and properties of some novel nonionic polyol surfactants. *J. Chem. Soc., Chem. Comm.* **1995**, *3*, 379–380.

(73) Bitha, P.; Child, R. G.; Hlavka, J. J.; Lin, Y.-I. Platinum Complexes of Amines with Dibasic Acids. U.S. Patent 4,675,336, 1987.

(74) Stroefer, E.; Rohr, W.; Rotermund, G. W.; Fischer, R.; Neudert, R. Preparation of 1-Pyrazolines. U.S. Patent 4,788,293, 1988.

(75) http://www.cyprotex.com/cloescreen/protein_binding/plasma-protein-binding/.

(76) The anesthetized guinea pig model is thought to be a predictive model for ECG changes in man, particularly that on QTc interval changes: (a) Hey, J. A.; Pardo, M. D.; Sherwood, J.; Kreutner, W.; Egan, R. W. Comparative analysis of the cardiotoxic proclivities of second generation antihistamines in an experimental model of adverse clinical ECG effects. *Arzneim. Forsch.* **1996**, *46*, 153–158. (b) Hey, J. A.; Pardo, M. D.; Kreutner, W.; Egan, R. W. Cardiotoxic and drug interaction profile of the second generation antihistamines ebastine and terfenadine in an experimental animal model of torsade de pointes. *Arzneim. Forsch.* **1996**, *46*, 159–163. In the meantime it has been shown that the use of telemetry transducers enables investigation of potential test substance effect in the absence of anesthesia in freely moving animals.

(77) Read, K. D.; Braggio, S. Assessing brain free fraction in early drug discovery. *Expert Opin. Drug Metab. Toxicol.* **2010**, *6*, 337–344.

(78) de Bruin, N. M. W. J.; Prickaerts, J.; van Loevezijn, A.; Venhorst, J.; de Groote, L.; Houba, P.; Reneerkens, O.; Akkerman, S.; Kruse, C. G. Two novel 5-HT_6 receptor antagonists ameliorate scopolamine-induced memory deficits in the object recognition and object location tasks in Wistar rats. *Neurobiol. Learn. Mem.* **2011**, *96*, 392–402.

(79) Spek, A. L. Single-crystal structure validation with the program PLATON. *J. Appl. Crystallogr.* **2003**, *36*, 7–13.

(80) Schinkel, A. H.; Wagenaar, E.; van Deemter, L.; Mol, C. A.; Borst, P. Absence of the mdr1a P-glycoprotein in mice affects tissue distribution and pharmacokinetics of dexamethasone, digoxin, and cyclosporin A. *J. Clin. Invest* **1995**, *96*, 1698–1705.

(81) Cherezov, V.; Rosenbaum, D. M.; Hanson, M. A.; Rasmussen, S. G.; Thian, F. S.; Kobilka, T. S.; Choi, H. J.; Kuhn, P.; Weis, W. I.; Kobilka, B. K.; Stevens, R. C. High-resolution crystal structure of an

engineered human β2-adrenergic G protein-coupled receptor. *Science* **2007**, *318*, 1258–1265.

(82) Okada, T.; Sugihara, M.; Bondar, A. N.; Elstner, M.; Entel, P.; Buss, V. The retinal conformation and its environment in rhodopsin in light of a new 2.2 Å crystal structure. *J. Mol. Biol.* **2004**, *342*, 571–583.

(83) Deupi, X.; Olivella, M.; Govaerts, C.; Ballesteros, J. A.; Campillo, M.; Pardo, L. Ser and Thr residues modulate the conformation of proline kinked transmembrane alpha-helices. *Biophys. J.* **2004**, *86*, 105–115.

(84) http://www.schrodinger.com.

(85) Boess, F. G.; Monsma, F. J., Jr.; Meyer, V.; Zwingelstein, C.; Sleight, A. J. Interaction of tryptamine and ergoline compounds with threonine 196 in the ligand binding site of the 5-hydroxytryptamine$_6$ receptor. *Mol. Pharmacol.* **1997**, *52*, 515–523.

(86) de la Fuente, T.; Martín-Fontecha, M.; Sallander, J.; Benhamú, B.; Campillo, M.; Medina, R. A.; Pellissier, L. P.; Claeysen, S.; Dumuis, A.; Pardo, L.; López-Rodríguez, M. L. Benzimidazole derivatives as new serotonin 5-HT$_6$ receptor antagonists. Molecular mechanisms of receptor inactivation. *J. Med. Chem.* **2010**, *53*, 1357–1369.

(87) Jones, G.; Willett, P.; Glen, R. C.; Leach, A. R.; Taylor, R. Development and validation of a genetic algorithm for flexible docking. *J. Mol. Biol.* **1997**, *267*, 727–748.

(88) Bazett, H. C. An analysis of the time relations of the electrocardiograms. *Heart* **1920**, *7*, 353–370.

(89) Liu, X.; Van Natta, K.; Yeo, H.; Vilenski, O.; Weller, P. E.; Worboys, P. D.; Monshouwer, M. Unbound drug concentration in brain homogenate and cerebral spinal fluid at steady state as a surrogate for unbound concentration in brain interstitial fluid. *Drug Metab. Dispos.* **2009**, *37*, 787–793.